Struct Multidisc Optim (2006) 32: 347–368
DOI 10.1007/s00158-005-0599-9

RESEARCH PAPER

C. Graczykowski · T. Lewiński

Michell cantilevers constructed within trapezoidal domains—Part I: geometry of Hencky nets

Received: 13 May 2005 / Revised manuscript received: 20 September 2005 / Published online: 10 June 2006

Abstract The present paper is the first part of the four-part work on Michell cantilevers transmitting a given point load to a given segment of a straight-line support, the feasible domain being a part of the half-plane contained between two fixed half-lines. The axial stress σ in the optimal cantilevers is assumed to be bounded by $-\sigma_C \leq \sigma \leq \sigma_T$, where σ_C and σ_T represent the allowable compressive and tensile stresses, respectively. The work provides generalization of the results of the article of Lewiński et al. (Int J Mech Sci 36:375–398, 1994a) to the case of $\sigma_T \neq \sigma_C$. The present, first part of the work concerns the analytical formation of the Hencky nets or the lines of fibres filling up the interior of the optimal cantilevers corresponding to an arbitrary position of the point of application of the given concentrated force.

Key words Michell structures · Hencky nets · minimum weight design · topology optimization · trusses

1 Introduction

The plane Michell structure is the lightest fully stressed structure contained within a certain feasible domain, transmitting a given load to a given line segment of a fixed support. The condition of the stresses being shifted to their extremes can be weakened without changing the optimal shape by assuming only that the stresses lie within the imposed limits $-\sigma_C \leq \sigma \leq \sigma_T$ because in the optimal structures considered, the stresses achieve their extreme values $-\sigma_C$ at compression and σ_T at tension. We assume that the density of mass is constant. Then, the condition of minimal weight is equivalent to the condition of minimal volume.

The original Michell (1904) structures have been thoroughly considered by Hemp (1973). In these structures the feasible or design domain is a plane or a half-plane. All the Michell results are correct if $\sigma_T = \sigma_C$. In a general case of $\sigma_T \neq \sigma_C$ the problems become much more difficult. A part of Michell's suggestions for that case is wrong, as pointed out by Rozvany (1997a) (see also Selyugin 2004). Michell's criteria for unequal permissible stresses are valid only for certain support conditions (cf. Rozvany 1997a). Any solution to a Michell problem consists of data of geometrical nature (geometry of fibres and reinforcing ribs) and of statical nature (distribution of stress resultants within the structure and in the reinforcing ribs); they both contribute to the final formula for the optimal weight. Moreover, the Michell problems can be formulated in two manners: primal and dual. In the primal formulation the statically admissible stress resultants [or rather their rates, by analogy with the theory of locking materials (see Lewiński and Telega 2001)] are the unknowns. In the dual problem the role of the unknowns is played by the virtual displacements. Both formulations have been discussed in the papers by Strang and Kohn (1983), Lewiński and Telega (2000, 2001), Lewiński (2004) and Graczykowski and Lewiński (2005). A problem can be viewed as solved if the results of both the formulations coincide. Then we say that the duality gap is zero. Although apparently important, this verification is uncommon in the literature; it was done for some elementary problems in Hemp (1973), for the twisted shells (in which $\sigma_T = \sigma_C$) in Lewiński (2004) and for the original Michell cantilever supported around the circle (see Graczykowski and Lewiński 2003, 2005). Let us emphasize here that other known solutions have not been verified in this respect till now.

An important problem of designing a cantilever supported along a straight line was solved by H.S.Y. Chan for the special case of $\sigma_T = \sigma_C$ (see Hemp 1973) by using a specific Hencky net discussed by Hill (1950) in the context of perfect plasticity. In the present paper we shall generalize this solution to the case of $\sigma_T \neq \sigma_C$, and we shall discuss its statical aspect. We shall put forward the distribution of stress resultants within the optimal cantilever and in the reinforc-

C. Graczykowski (✉)
Institute of Fundamental Technological Research,
Polish Academy of Sciences,
Świętokrzyska 21, 00-049, Warsaw, Poland
e-mail: Cezary.Graczykowski@ippt.gov.pl

T. Lewiński
Faculty of Civil Engineering, Institute of Structural Mechanics,
Warsaw University of Technology,
al.Armii Ludowej 16, 00-637, Warsaw, Poland
e-mail: T.Lewinski@il.pw.edu.pl

ing bars. The first sketches of the optimal layout of fibres for the case of $\sigma_T \neq \sigma_C$ were already given by Prager (1959) and Rozvany (1997a). However, no mathematical formulae were derived there. A correct two-bar solution was first presented by Rozvany (1997a). In the present paper (part IV), for the first time, a proof of the duality gap being zero is provided.

Important suboptimal solutions refer to the cantilevers designed within certain subdomains of the half-plane, e.g., those included between the half-lines starting at the end points of a given supporting line segment. In the case of $\sigma_T = \sigma_C$ such cantilevers were constructed by Chan (1967). Their extensions, referring to the concentrated loads applied at points lying at bigger distances from the support, have been proposed in the paper by Lewiński et al. (1994a), where the analysis has been confined to the kinematic and geometric facets, the distribution of stress resultants being not discussed.

The aim of the present four-part paper is at

i.) Completing the analysis of cantilevers given in the papers by Chan (1967) and Lewiński et al. (1994a) by adding information on distribution of the internal force fields;
ii.) Generalization of all the known constructions to the case of $\sigma_T \neq \sigma_C$;
iii.) Confirming the correctness of the final results by showing that both the approaches, kinematic and static, lead to identical results for the weights of the optimal structures;
iv.) Consideration of sequences of trusses (of finite number of nodes) tending to the ideal discrete-continuous solutions, showing that the sequences of weights tend to the theoretical predictions of weights of the ideal solutions (given by explicit analytical formulae).

The paper consists of four parts. The present, first part presents construction of the relevant Hencky nets. The second part deals with the virtual displacement fields relevant to the net found. The static analysis is put forward in the third part of the paper. The final formulae for the weights of optimal cantilevers will be derived in the last part, where some examples will also be given with all details. The analytical results will be checked by the method of Prager (1978a,b) by considering special trusses of finite number of joints. The numerical results contained in part IV will be useful as a benchmarks for numerical solutions of topological optimization problems.

The present paper extends the results of the works of Lewiński et al. (1994a,b). To make the references to this work possibly brief, we shall write, e.g., (a.102) and Section a.6 to refer to (102) and Section 6 of Lewiński et al. (1994a), respectively, and write (b.161) and Section (b.7) instead of writing (161) and Section 7 of Lewiński et al. (1994b), respectively. On the other hand, the information (A1) refers to (A.1) in the Appendix A of the present paper.

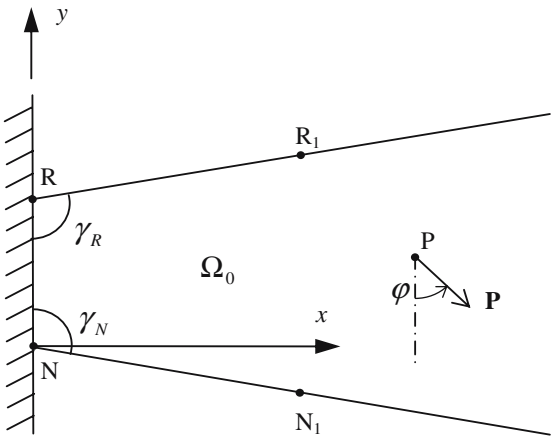

Fig. 1 Geometry of the feasible domain Ω_0 and position P of the application of the point load

2 Michell cantilever problem

Consider the domain Ω_0 bounded by the straight segment RN and the half-lines RR_1, NN_1 (see Fig. 1). This domain is parameterized by an orthogonal Cartesian system (x, y). An arbitrary point of this domain is also denoted by (x, y). Along RN the structure to be constructed should be fixed with no sliding, but not all the points of RN should necessarily be used as supporting points.

The domain Ω_0 will be called trapezoidal because it can be made finite by cutting it by a straight line parallel to RN, going through the point P of application of the concentrated force **P**. The stress state is viewed as admissible if the axial stress along all directions satisfy

$$-\sigma_C \leq \sigma \leq \sigma_T, \tag{2.1}$$

where $-\sigma_C$, σ_T are limit values at compression and tension, respectively. The problem is to form the lightest structure, admissibly stressed according to (2.1), transmitting a given point load **P** of magnitude P to the support RN. The force **P** is get out of plumb by angle φ (see Fig. 1). The available literature of the subject teaches us that the lightest cantilever will have a discrete-continuous structure: its interior Ω, $\Omega \subset \Omega_0$, is made of a net of orthogonal fibres transmitting compression or tension, while its edge is reinforced by two ribs also compressed and tensioned; the ribs cannot undergo bending and transverse shearing. The curvilinear reinforcing ribs RP and NP encompass the finite domain Ω within the infinite feasible domain Ω_0. The ribs must join at the point P of application of the force **P**. The force **P** is equilibrated by the tensile force F_T in one rib and the compressive force F_C in the second rib. The units of these forces are newtons (N). In general, these forces vary along the ribs, which is denoted as $F_T = F_T(s)$ and $F_C = F_C(s)$, where s is the natural parameter of the boundary lines.

The ribs are subject to a distributed normal loading N_n and tangent loading N_τ, acting from within the interior domain Ω (Fig. 2). Within Ω the state of stress obeys the plane stress assumptions. The state of stress in Ω is determined by the

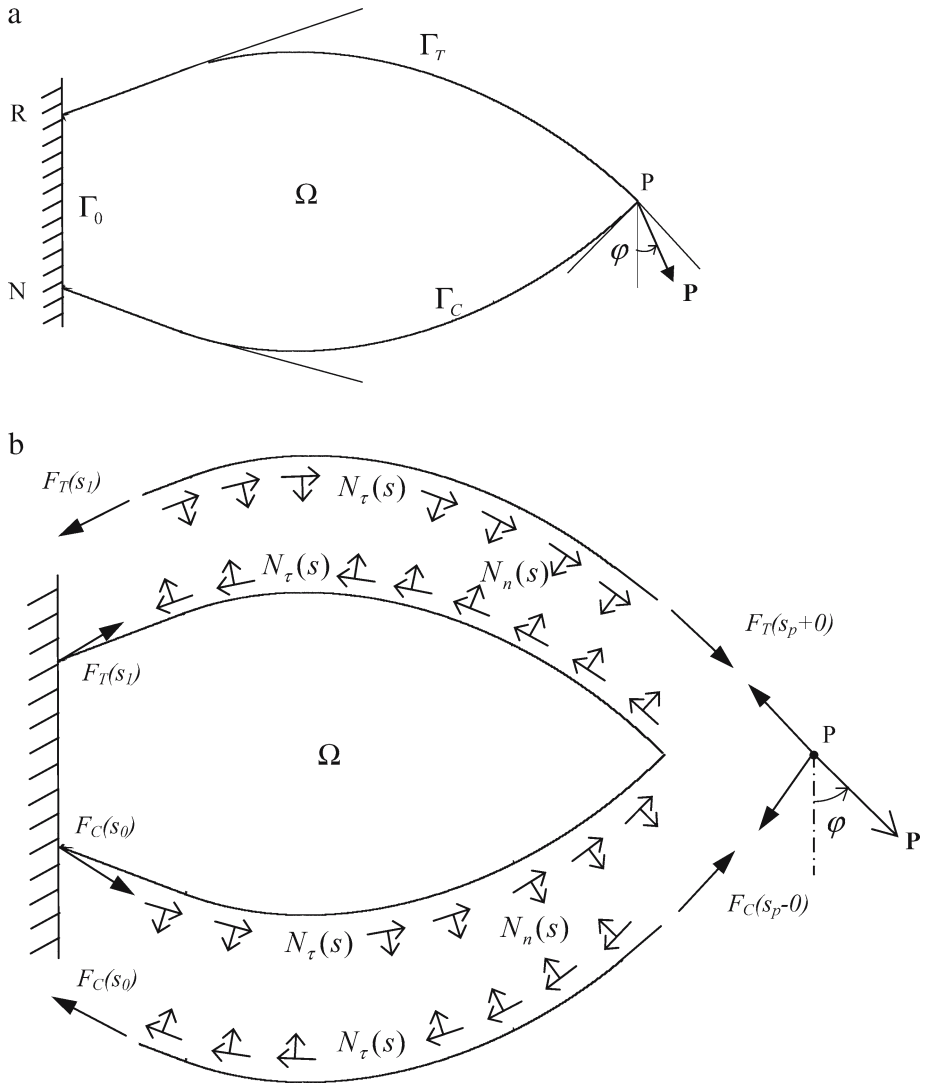

Fig. 2 The cantilever problem. **a** The cantilever reinforced by ribs; **b** decomposition of the structure into the interior, ribs and the node P

tensor field $\mathbf{N} = \left(N^{\gamma\delta}\right)$, with γ, δ=1,2, of stress resultants. The principal stress resultants are denoted by N_{I}, N_{II}. The units of the quantities $N^{\alpha\beta}$, N_{I}, N_{II}, are newtons per meter. The tangent and normal stress resultants along Γ_T and Γ_C are denoted by N_τ, N_n, respectively.

We say that the triple $(\mathbf{N}, F_T, F_C)$ is statically admissible and write $(\mathbf{N}, F_T, F_C) \in \Sigma\left(\overline{\Omega}\right)$ if the following equations are satisfied:

(a) Two algebraic equilibrium equations of the node P
(b) Differential equilibrium equations of the ribs:

$$\frac{dF}{ds} - N_\tau(s) = 0, \quad \frac{F(s)}{R(s)} + N_n(s) = 0 \ \text{ on } \ \Gamma, \tag{2.2}$$

where F=F_T or F_C; R represents the radius of curvature of the boundary line Γ, Γ=Γ_T or Γ=Γ_C.

Note that the ribs do not sustain bending and transverse shearing, and their equilibrium is only possible if they are curved whenever N_n does not vanish.

c) $\operatorname{div} \mathbf{N} = 0$ in Ω (2.3)

or the differential equilibrium equations of the interior part of the structure.The set $\Sigma\left(\overline{\Omega}\right)$ is affine and does not have properties of a function space because equations (a) are inhomogeneous.

To express the conditions (a–c) by one variational equilibrium equation we introduce a trial displacement field $\overline{\mathbf{u}}$ into the domain Ω_0. Let $\overline{u}_n$, $\overline{u}_\tau$ denote the components of $\overline{\mathbf{u}}$ normal and tangent to Γ_C, Γ_T. Along the contours Γ_C, Γ_T we define the operator

$$\varepsilon_\Gamma(\overline{\mathbf{u}}) = \frac{d\overline{u}_\tau}{ds} + \frac{\overline{u}_n(s)}{R(s)}, \tag{2.4}$$

which determines elongation along the contour, associated with the field $\overline{\mathbf{u}}$. Moreover, the quantity $\varepsilon(\overline{\mathbf{u}})$ represents the

strain field associated with $\overline{\mathbf{u}}$, defined as the symmetric part of the gradient. Let $U(\overline{\Omega})$ be the set of kinematically admissible $\overline{\mathbf{u}}$ given within $\overline{\Omega}$. We require here that $\overline{\mathbf{u}} = 0$ on Γ_0 = NR, and that the field $\overline{\mathbf{u}}$ is continuous in $\overline{\Omega}$; hence, the set $U(\overline{\Omega})$ is a space. The vector field $\overline{\mathbf{u}}_{|\Gamma}$ determines the displacements of the reinforcing ribs. Thus, the reinforcing ribs cannot slide along the boundary of the domain. The regularity assumptions of the field $\overline{\mathbf{u}}$ will not be discussed.

One can prove that the triple $(\widetilde{\mathbf{N}}, \widetilde{F}_T, \widetilde{F}_C)$ is statically admissible or

$$(\widetilde{\mathbf{N}}, \widetilde{F}_T, \widetilde{F}_C) \in \Sigma(\overline{\Omega}) \quad \text{if}$$

$$\int_\Omega \widetilde{\mathbf{N}} : \boldsymbol{\varepsilon}(\overline{\mathbf{u}}) dxdy + \int_{\Gamma_T} \widetilde{F}_T \varepsilon_\Gamma(\overline{\mathbf{u}}) ds + \int_{\Gamma_C} \widetilde{F}_C \varepsilon_\Gamma(\overline{\mathbf{u}}) ds = \mathbf{P} \cdot \overline{\mathbf{u}}(\mathrm{P})$$

$$\text{for each } \overline{\mathbf{u}} \in U(\overline{\Omega}). \tag{2.5}$$

Here, the product : means the full contraction.

We assume that the tension fibres and the tension rib RP are fully stressed and there $\sigma = \sigma_T$, while in the compressed fibres and in the compression rib NP the stresses are $\sigma = -\sigma_C$. The volume of the material used for constructing such a discrete-continuous structure is expressed by the formula

$$V_\Omega = I(\mathbf{N}, F_T, F_C; \overline{\Omega}), \tag{2.6}$$

where

$$I(\mathbf{N}, F_T, F_C; \overline{\Omega}) = \int_\Omega \left(\frac{1}{\sigma_T} |N_I| + \frac{1}{\sigma_C} |N_{II}| \right) dxdy + \int_{\Gamma_T} \frac{1}{\sigma_T} |F_T| ds + \int_{\Gamma_C} \frac{1}{\sigma_C} |F_C| ds. \tag{2.7}$$

The form of the first component of (2.7) was justified in Lewiński (2004; Section 4); the remaining components have an obvious form. If γ=const is the weight density of the material, then $Q = \gamma V_\Omega$ is the weight of the structure. Then the problems of minimizing the weight and the volume are equivalent. The fields $\mathbf{N}, F_T, F_C$ are linked by the equilibrium conditions (of the fibrous domain, of ribs and of the node P). The formula (2.6) can be rewritten as follows:

$$V_\Omega = \min \left\{ I(\widetilde{\mathbf{N}}, \widetilde{F}_T, \widetilde{F}_C; \overline{\Omega}) \,|\, (\widetilde{\mathbf{N}}, \widetilde{F}_T, \widetilde{F}_C) \in \Sigma(\overline{\Omega}) \right\} \tag{2.8}$$

because it occurs that the optimal cantilever is statically determinate, or the set $\Sigma(\overline{\Omega})$ for such a selected domain Ω contains only one element, thus making the formulae (2.6) and (2.8) equivalent. The feature of statical determinacy will be cleared up in part III of the present paper and will be reflected in statical determinacy of the approximating trusses (see part IV).

The minimum volume problem (2.8) can be transformed into a dual form

$$V_\Omega = \frac{1}{\sigma_T} \max \{ \mathbf{P} \cdot \overline{\mathbf{u}}(\mathrm{P}) \,|\, \overline{\mathbf{u}} \in U(\overline{\Omega}), \quad \boldsymbol{\varepsilon}(\overline{\mathbf{u}})(x, y) \in B_\kappa, \quad (x, y) \in \Omega, -\kappa \le \varepsilon_\Gamma(\overline{\mathbf{u}}) \le 1 \text{ on } \Gamma_T, \Gamma_C \}, \tag{2.9}$$

where $\kappa = \sigma_T / \sigma_C$ and

$$B_\kappa = \left\{ \boldsymbol{\varepsilon} \in E_s^2 \,|\, |\varepsilon_I| \le 1, |\varepsilon_{II}| \le \kappa \right\}. \tag{2.10}$$

Here, E_s^2 represents the set of symmetric second-order tensors.

A passage from the problem (2.8) to (2.9) goes according to the lines of a similar passage shown in the paper by Strang and Kohn (1983) for the cases when the two last components of (2.7) are absent (cf. Lewiński 2004). Thus, the derivation of (2.9) can be omitted here. In the problem considered here, minimum in (2.8) is achieved for the domain $\widetilde{\Omega} = \Omega$, the boundary lines of which, Γ_T, Γ_C, lie along the trajectories of the principal strains $\varepsilon_I(\overline{\mathbf{u}})$, $\varepsilon_{II}(\overline{\mathbf{u}})$. Then the condition $-\kappa \le \varepsilon_\Gamma(\overline{\mathbf{u}}) \le 1$ is satisfied along the boundary in the following way: $\varepsilon_\Gamma(\overline{\mathbf{u}}) = 1$ on Γ_T and $\varepsilon_\Gamma(\overline{\mathbf{u}}) = -\kappa$ on Γ_C. The field $\boldsymbol{\varepsilon}(\overline{\mathbf{u}})$ is defined on $\overline{\Omega}$, and thus, can be determined along its boundary or along Γ_T, Γ_C. Thus, the conditions $\varepsilon_\Gamma(\overline{\mathbf{u}}) = 1$ on Γ_T and $\varepsilon_\Gamma(\overline{\mathbf{u}}) = -\kappa$ on Γ_C can be rewritten as $\varepsilon_I(\overline{\mathbf{u}}) = 1$ on Γ_T and $\varepsilon_{II}(\overline{\mathbf{u}}) = -\kappa$ on Γ_C. According to this remark problem (2.9) can be put in the form

$$V_\Omega = \frac{1}{\sigma_T} \max \{ \mathbf{P} \cdot \overline{\mathbf{u}}(\mathrm{P}) \,|\, \overline{\mathbf{u}} \in U(\Omega), \boldsymbol{\varepsilon}(\overline{\mathbf{u}})(x, y) \in B_\kappa, (x, y) \in \overline{\Omega} \} \tag{2.11}$$

provided that the boundary lines RP, NP lie along trajectories of principal strains.

Having now the formulation (2.11) one step of generalization is possible. One can make the formulation free from the choice of Ω! Indeed, let $U(\Omega_0)$ represent the function space of such displacements which vanish on Γ_0=RN. Consider the problem

$$V = \frac{1}{\sigma_T} \max \{ \mathbf{P} \cdot \overline{\mathbf{u}}(\mathrm{P}) \,|\, \overline{\mathbf{u}} \in U(\Omega_0), \boldsymbol{\varepsilon}(\overline{\mathbf{u}})(x, y) \in B_\kappa, (x, y) \in \Omega_0 \}, \tag{2.12}$$

which determines a volume V not referring to any particular domain Ω. In the problems analysed in the present paper both the formulations (2.11) and (2.12) are equivalent because $\overline{\Omega}$ in (2.11) is not arbitrary. It contains Γ_0=RN, and its boundaries RP, RN are in fact determined by the trajectories of the virtual strain field. The formulation (2.12) is much simpler than (2.8) because it involves maximization over one field $\overline{\mathbf{u}}$. In this paper the volume will be computed by both the formulae (2.8) and (2.12). The formula (2.8) will be used in the form (2.7) upon finding the stress resultants within Ω and in the ribs. Such a test verifies all the results and additionally provides distribution of the fibres within Ω. Their density per unit area is expressed by

$$h = \frac{1}{\sigma_T} |N_I| + \frac{1}{\sigma_C} |N_{II}|. \tag{2.13}$$

This quantity is sometimes interpreted as an effective thickness of the plate (see Hemp 1973). In the all-optimal solutions considered in the present paper maximum in (2.12) is achieved if

$$\varepsilon_I(\overline{\mathbf{u}}) = 1, \quad \varepsilon_{II}(\overline{\mathbf{u}}) = -\kappa \tag{2.14}$$

in each point of Ω_0. Along the ribs one has

$$\varepsilon_\Gamma(\overline{\mathbf{u}}) = 1 \text{ on } \Gamma_T \text{ and } \varepsilon_\Gamma(\overline{\mathbf{u}}) = -\kappa \text{ on } \Gamma_C. \tag{2.15}$$

The conditions (2.14) can hold only in specific curvilinear systems called Hencky nets. These nets determine the lines of fibres within the domain Ω bounded by the ribs Γ_T and Γ_C.

3 Geometry of Hencky nets corresponding to the conditions: $\varepsilon_I(\overline{\mathbf{u}}) = 1$ and $\varepsilon_{II}(\overline{\mathbf{u}}) = -\kappa$

The necessary geometric formulae can be found in Hemp (1973) and Lewiński et al. (1994a). Thus, we shall quote here only those of the formulae which are indispensable for further analysis.

The conditions (2.14) can be satisfied only along the parametric lines of very specific curvilinear orthogonal systems.

Let (x, y) be the Cartesian parameterization; the lines α=const and β=const form the unknown orthogonal system of parametric lines (see Fig. 3) given by the equations $x=x(\alpha, \beta)$, $y=y(\alpha, \beta)$.

In a standard manner we introduce the metric tensor of components denoted by $(g_{\gamma\delta})$. Due to orthogonality we introduce the Lamé coefficients $A(\alpha, \beta)$, $B(\alpha, \beta)$ as follows:

$$g_{11} = A^2(\alpha, \beta), \quad g_{12} = 0, \quad g_{22} = B^2(\alpha, \beta) \tag{3.1}$$

and adopt the convention of A and B being of length dimension. Let $\phi(\alpha, \beta)$ be an angle between the tangent to the line α at point (α, β) and the axis x (cf. Fig. 3). If the fields $A(\alpha, \beta), B(\alpha, \beta)$ are given, the parametric lines of the system

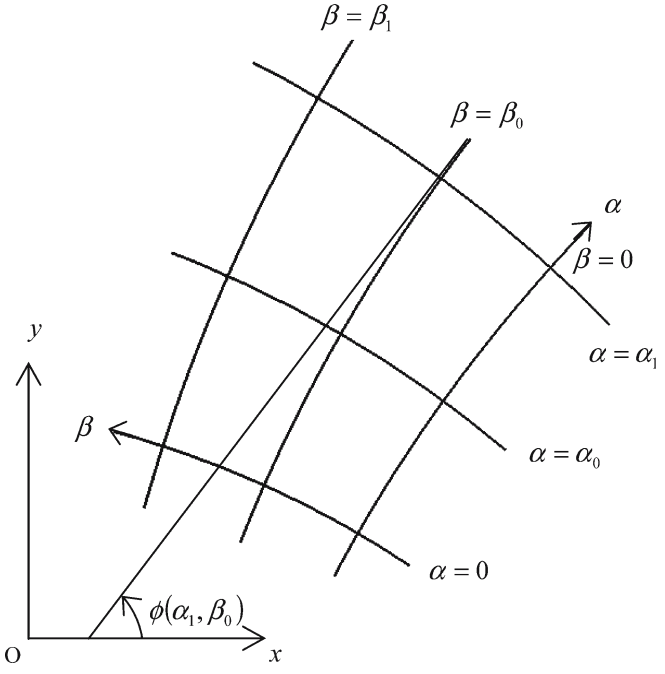

Fig. 3 The curvilinear system (α, β)

(α, β) are determined by the equations giving the Cartesian coordinates (x, y) of an arbitrary point $\alpha=\lambda$, $\beta=\mu$

$$\begin{aligned} x(\lambda, \mu) = x^0 &+ \int_0^\lambda \cos\phi(\alpha, \mu) A(\alpha, \mu) d\alpha \\ &- \int_0^\mu \sin\phi(\lambda, \beta) B(\lambda, \beta) d\beta \\ y(\lambda, \mu) = y^0 &+ \int_0^\lambda \sin\phi(\alpha, \mu) A(\alpha, \mu) d\alpha \\ &+ \int_0^\mu \cos\phi(\lambda, \beta) B(\lambda, \beta) d\beta, \end{aligned} \tag{3.2}$$

where (x^0, y^0) is a point of coordinates $\alpha=0$, $\beta=0$. In this paper we consider the nets characterized by the formula (see Hemp 1973)

$$\phi(\alpha, \beta) = \phi_0 + \hat{b}\beta - \hat{a}\alpha, \tag{3.3}$$

where $\phi_0, \hat{b}, \hat{a}$ are constants. The formula above makes it possible to satisfy the optimality conditions (2.14) in all the optimization problems considered in the present paper.

One can prove that under the assumption (3.3) the Lamé coefficients are linked by (see Hemp 1973)

$$\frac{\partial A}{\partial \beta} = \hat{a}B, \quad \frac{\partial B}{\partial \alpha} = \hat{b}A \tag{3.4}$$

or

$$\frac{\partial^2 A}{\partial \alpha \partial \beta} - \hat{c}A = 0, \quad \frac{\partial^2 B}{\partial \alpha \partial \beta} - \hat{c}B = 0, \tag{3.5}$$

where $\hat{c} = \hat{b}\hat{a}$. In the problem considered the orthogonality of parametric lines holds. In general, the nonorthogonality can take place (see Rozvany 1997b).

4 The case of a position of the point P being close to the edge RN

We confine here our attention to the optimal cantilevers, the shapes of which are independent of the lines RR_1, NN_1 bounding the domain Ω_0. First, we find the positions of points P which generate such solutions. The problem thus posed can be reformulated to the form of the problem considered in Section 2, where Ω_0 is a half-plane at the right hand side of the line RN. From now onwards the Cartesian frame determined by the support RN will be denoted by x_0, y_0 (see Fig. 4). Now the feasible domain is included in the half-plane $x_0 \geq 0$. Distance of point P to the supporting line RN is denoted by d or $d=x_0$ (P).

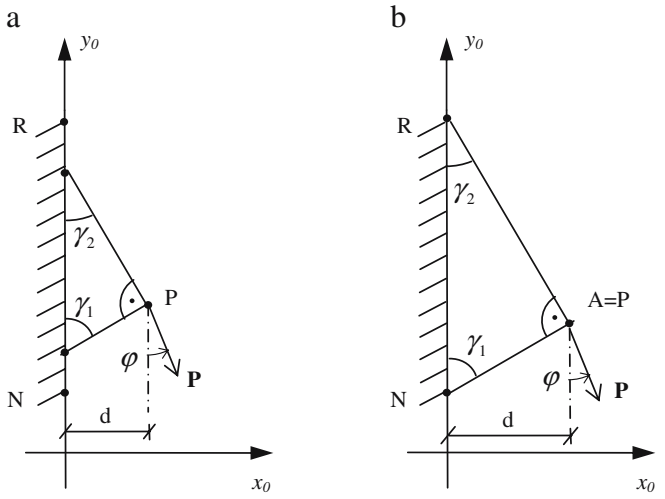

Fig. 4 Two-bar solutions. **a** Point P is close to the support; **b** the optimal two-bar truss of maximal dimensions

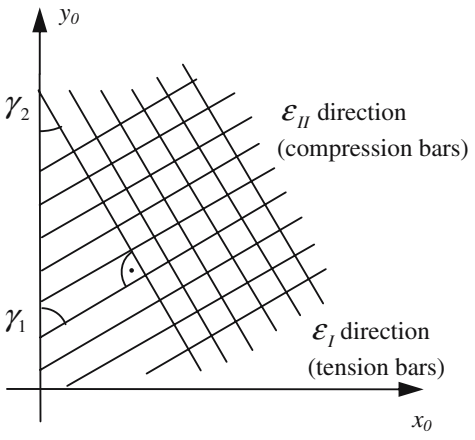

Fig. 5 Trajectories of virtual principal strains

The shape of the optimal structure depends heavily on the angle φ (see Fig. 1)

i.) If

$$-\arctan\kappa^{1/2} < \varphi < \arctan\kappa^{-1/2}, \tag{4.1}$$

then the optimal structure is a truss consisting of two bars, as shown in Fig. 4a; the angles of inclination of bars are determined by κ:

$$\gamma_1 = \arctan\left(\kappa^{1/2}\right),\ \gamma_2 = \arctan\left(\kappa^{-1/2}\right). \tag{4.2}$$

The bars are orthogonal.

ii.) If φ does not satisfy (4.1), then the optimal solution consists of one bar directed along the force.

The proof of (ii) will be omitted. We concentrate now on proving (i). First we construct the field of virtual displacements $\overline{\mathbf{u}} = \left(u_{x_0}, u_{y_0}\right)$, satisfying the conditions (2.14) for $x_0 \geq 0$. We predict the representations

$$u_{x_0} = \widetilde{a}x_0 + \widetilde{b}y_0 + \widetilde{c},\quad u_{y_0} = \widetilde{d}x_0 + \widetilde{e}y_0 + \widetilde{f} \tag{4.3}$$

and impose the conditions of kinematic admissibility: $u_{x_0}(0, y_0) = 0\ u_{y_0}(0, y_0) = 0$.

Hence, $u_{x_0} = \widetilde{a}x_0,\ u_{y_0} = \widetilde{d}x_0$. The representation of $\boldsymbol{\varepsilon}(\overline{\mathbf{u}})$ in the coordinates (x_0, y_0) has the form

$$\boldsymbol{\varepsilon}(\overline{\mathbf{u}}) = \begin{bmatrix} \widetilde{a} & \widetilde{d}/2 \\ \widetilde{d}/2 & 0 \end{bmatrix}. \tag{4.4}$$

The characteristic equation $\lambda^2 - \lambda\widetilde{a} - \widetilde{d}^2/4 = 0$ should have the roots equal to 1 or $-\kappa$; hence, $\widetilde{a} = 1 - \kappa$, $\widetilde{d} = \pm 2\kappa^{1/2}$. We compute the virtual work

$$\mathbf{P} \cdot \overline{\mathbf{u}}(\mathrm{P}) = P\left(u_{x_0}\sin\varphi - u_{y_0}\cos\varphi\right). \tag{4.5}$$

We choose $\widetilde{d} = -2\kappa^{1/2}$ to maximize the above expression to find

$$\mathbf{P} \cdot \overline{\mathbf{u}}(\mathrm{P}) = Pd\left((1-\kappa)\sin\varphi + 2\kappa^{1/2}\cos\varphi\right). \tag{4.6}$$

The unknown displacement field is of the form

$$u_{x_0} = (1-\kappa)x_0 \qquad u_{y_0} = -2\kappa^{1/2}x_0. \tag{4.7}$$

We compute now the angle of inclination of the principal strain by using the known formula

$$\tan 2\gamma_I = \frac{2\varepsilon_{xy}}{\varepsilon_x - \varepsilon_y}; \tag{4.8}$$

hence, $\gamma_I = -\arctan\left(\kappa^{1/2}\right)$ or $\gamma_I = -\gamma_1$. Moreover, $\gamma_{II} = \arctan\left(\kappa^{-1/2}\right)$ or $\gamma_{II} = \gamma_2$. The above results determine the Hencky net (see Fig. 5).

The two-bar solution holds good if the point of application of the force lies within the triangle RNA (Fig. 4). The lengths of the sides $r_1 = |\mathrm{NA}|,\ r_2 = |\mathrm{RA}|$ are

$$r_1/a = \cos\left(\arctan\kappa^{1/2}\right),\ r_2/a = \sin\left(\arctan\kappa^{1/2}\right), \tag{4.9}$$

where a=RN. Thus, we note that

$$r_2/r_1 = \kappa^{1/2}. \tag{4.10}$$

5 One-fan designs

Let us note that if point P lies within the domains of circular sections RBA, NAC (see Fig. 6), then the optimal structure consists of one fan reinforced by a rib which then stretches and runs straight to the supports at R and N. The notion *fan* means a fibrous plate composed of infinite number of infinitely thin bars going radially from one point. Both the fans appearing here have a circular boundary reinforced by cables of finite cross sections (or ribs in tension or compression, incapable of sustaining both bending and transverse shearing). Thus, the fans are discrete-continuous structures. The triangular domain RAN is now empty (or no bars lie inside).

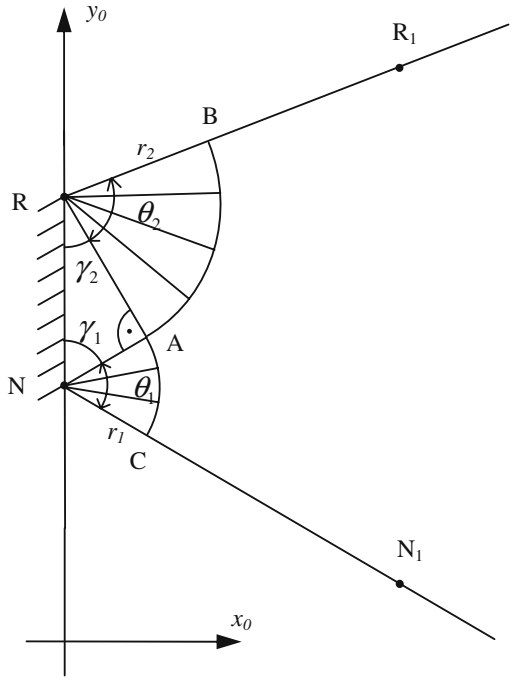

Fig. 6 Geometry of the fan domains

In the present section only the geometrical aspects of the nets will be dealt with. Position of point P in RBA is determined by α_1=RP/r_2 and by angle β (see Fig. 7).

The elementary lengths of the lines α_1, β are given by

$$ds_1 = d(r_2\alpha_1) = r_2 d\alpha_1, \qquad ds_2 = r_2\alpha_1 d\beta, \tag{5.1}$$

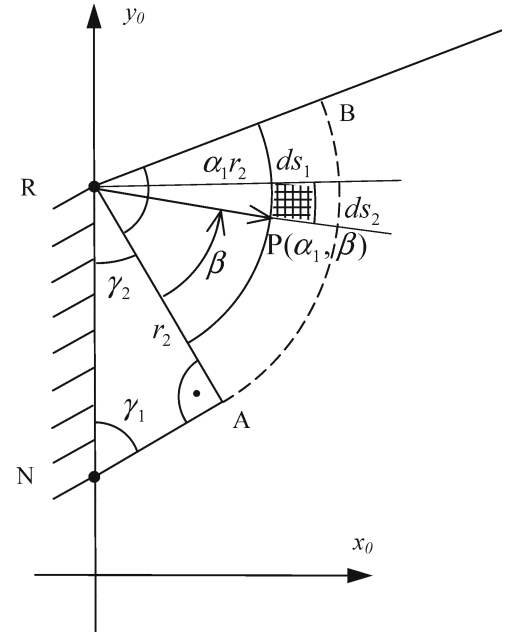

Fig. 7 Parameterization of the upper fan domain

or the Lamé coefficients are

$$A(\alpha_1, \beta) = r_2,$$

$$B(\alpha_1, \beta) = r_2\alpha_1 \quad 0 \le \alpha_1 \le 1, \quad 0 \le \beta \le \theta_2, \tag{5.2}$$

where θ_2=∠ (ARR$_1$) (see Fig. 6). Position of point P within the circular section NAC is given by NP=$r_1\beta_1$, $0 \le \beta_1 \le 1$ and by the angle α, $0 \le \alpha \le \theta_1$, where θ_1=∠ (ANN$_1$) (see Fig. 6). The elementary lengths along the parametric lines (Fig. 8) are

$$ds_1 = r_1\beta_1 d\alpha, \qquad ds_2 = r_1 d\beta_1, \tag{5.3}$$

or the Lamé coefficients are given by

$$A(\alpha, \beta_1) = r_1\beta_1, \qquad B(\alpha, \beta_1) = r_1. \tag{5.4}$$

The Hencky nets in RBA and NAC are constructed by the radial lines and by the circumferential lines (see Fig. 9).

In the domain RBA we have

$$\phi(\alpha_1, \beta) = \gamma_1 - \beta. \tag{5.5}$$

In the domain NAC

$$\phi(\alpha, \beta_1) = -\gamma_1 - \alpha. \tag{5.6}$$

Thus, the angle ϕ is expressed by (3.3) with appropriate constants $\phi_0, \hat{a}, \hat{b}$.

6 Prager–Hill designs

Consider the case of the position P of application of the force **P** at the right hand side of the arcs BA, AC, but within the domain ABDC; the shapes of the lines BD and CD will be given in the sequel.

The net of lines within ABDC, in case of κ=1, was found by Hill (1950) in the context of the plastic flow theory; the

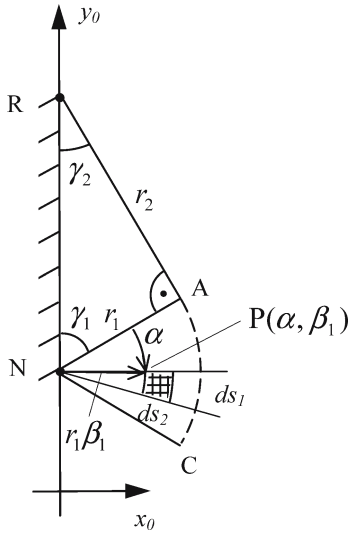

Fig. 8 Parameterization of the lower fan domain

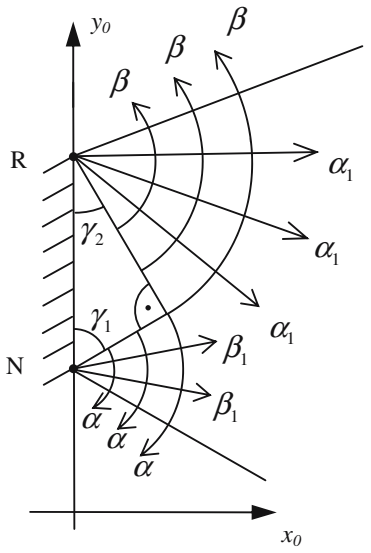

Fig. 9 Parameterization of both fan domains

result of Hill was used by Chan (1967) and Hemp (1973) for the construction of Michell nets. The case of $\kappa \neq 1$ was considered by Prager (1959), but in the mentioned paper, no analytical formulae were given. The formulae given below have never been published before. The construction of the Hencky net based on two circles of different radii can be found in Section 4 of the report: H.S.Y. Chan, Tabulation of some layouts and virtual displacement fields in the theory of Michell optimum structures. CoA Note Aero No 161. Febr. 1964, the College of Aeronautics. Dept. of Aircraft Design.

These results refer to the case of $\kappa = 1$, hence were not motivated by the problem considered in this paper.

The Hencky net will be constructed in the Cartesian orthogonal system (x, y) as in Fig. 10. According to the results of Hill (1950) and Chan (1967) the function $\phi\,(\alpha, \beta)$ is represented as follows:

$$\phi(\alpha, \beta) = \beta - \alpha \tag{6.1}$$

or $\hat{a} = 1$, $\hat{b} = 1$. The above representation determines the fields $A(\alpha, \beta)$, $B(\alpha, \beta)$ within the domain ABDC because these fields are linked by (3.4); hence,

$$\frac{\partial A}{\partial \beta} = B, \quad \frac{\partial B}{\partial \alpha} = A, \quad LA = 0, \quad LB = 0, \tag{6.2}$$

where

$$L = \frac{\partial^2}{\partial \alpha \partial \beta} - 1 \tag{6.3}$$

with the following conditions along the circular boundaries:

$$A(\alpha, 0) = r_1 \quad (\text{line AC}), \quad B(0, \beta) = r_2 \quad (\text{line BA})\,. \tag{6.4}$$

Thus, the net (α, β) is constructed by starting from finding the fields A, B. We use the formula of Riemann (see (a.17)) to find

$$A(\lambda, \mu) = A(0, 0) \cdot G_0(\lambda, \mu) + \int_0^{\lambda} G_0(\lambda - \alpha, \mu) \frac{\partial A(\alpha, 0)}{\partial \alpha} d\alpha$$

$$+ \int_0^{\mu} G_0(\lambda, \mu - \beta) \frac{\partial A(0, \beta)}{\partial \beta} d\beta, \tag{6.5}$$

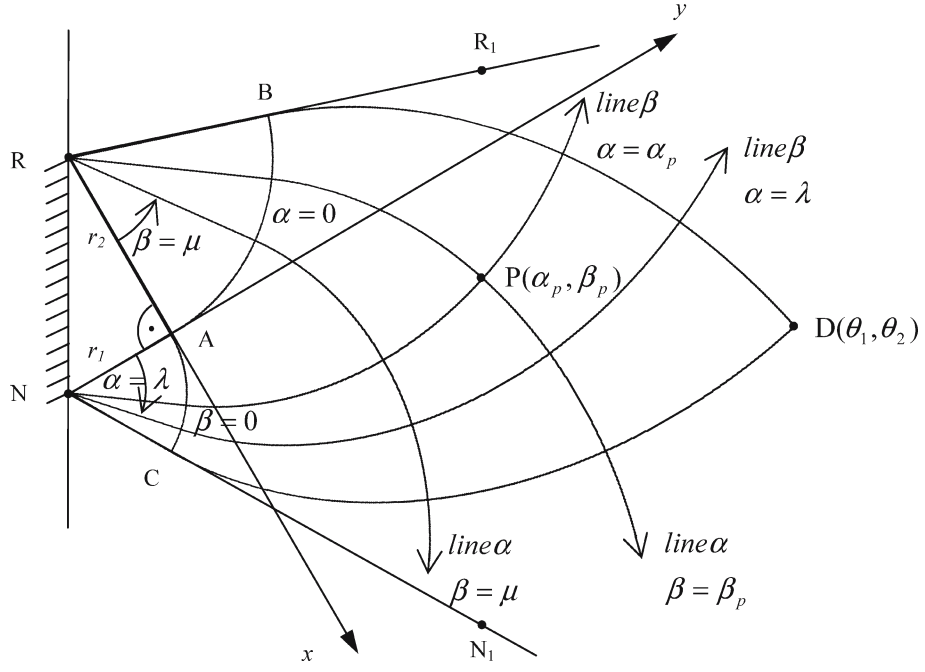

Fig. 10 Prager-Hill problem. The Cartesian frame (x,y) is now inclined to the supporting line RN. Here, $\angle$BRA=θ_2, $\angle$ANC=θ_1.

where $G_0\ (\alpha,\ \beta)=I_0\ [2(\alpha\beta)^{1/2}]$, $I_0\ (x)$ being the modified Bessel function (see (a.3)). We shall make use also of functions $G_n\ (\alpha,\beta)$, $n=0,\pm1,\pm2,...$ defined in Section a.2, and we shall use their properties given therein; they will not be repeated here.

Upon taking into account (6.2) and (6.3) we arrive at

$$A(\lambda,\mu)=r_1G_0(\lambda,\mu)+r_2\int_0^{\mu}G_0(\lambda,\mu-\beta)d\beta. \tag{6.6}$$

By using (a.4) and (a.14) we find

$$A(\lambda,\mu)=r_1G_0(\lambda,\mu)+r_2G_1(\mu,\lambda). \tag{6.7}$$

According to (6.2) $B=\partial A(\lambda,\mu)\big/\partial\mu$. Using the differential rules (a.4) we find

$$B(\lambda,\mu)=r_2G_0(\lambda,\mu)+r_1G_1(\lambda,\mu). \tag{6.8}$$

One can check that the field B found in this manner satisfies (6.4) on BA [see the properties (a.14)]. Thus, we find both the fields $A(\alpha,\beta)$, $B(\alpha,\beta)$, which makes the construction of the lines (α,β) possible. To this end we use the integral formulae (3.2) along the line β=const. Taking into account (6.1) we write

$$\begin{aligned}x(\lambda,\mu)&=x(0,\mu)+\int_0^{\lambda}\cos(\mu-\alpha)A(\alpha,\mu)d\alpha\\ y(\lambda,\mu)&=y(0,\mu)+\int_0^{\lambda}\sin(\mu-\alpha)A(\alpha,\mu)d\alpha.\end{aligned} \tag{6.9}$$

To make the integration possibly easy we introduce new unknowns called Mikhlin unknowns (see Hill 1950, Section 5, chap. VI) and (a.54):

$$\begin{aligned}\overline{x}(\lambda,\mu)&=x(\lambda,\mu)\cos(\mu-\lambda)+y(\lambda,\mu)\sin(\mu-\lambda)\\ \overline{y}(\lambda,\mu)&=-x(\lambda,\mu)\sin(\mu-\lambda)+y(\lambda,\mu)\cos(\mu-\lambda)\end{aligned} \tag{6.10}$$

and rewrite (6.9) in the form

$$\begin{aligned}\overline{x}(\lambda,\mu)&=\widetilde{x}(\lambda,\mu)+\int_0^{\lambda}\cos(\lambda-\alpha)A(\alpha,\mu)d\alpha\\ \overline{y}(\lambda,\mu)&=\widetilde{y}(\lambda,\mu)+\int_0^{\lambda}\sin(\lambda-\alpha)A(\alpha,\mu)d\alpha,\end{aligned} \tag{6.11}$$

where

$$\begin{aligned}\widetilde{x}(\lambda,\mu)&=\cos(\lambda-\mu)x(0,\mu)+\sin(\mu-\lambda)y(0,\mu)\\ \widetilde{y}(\lambda,\mu)&=-\sin(\mu-\lambda)x(0,\mu)+\cos(\mu-\lambda)y(0,\mu).\end{aligned} \tag{6.12}$$

The coordinates of the point $(0,\mu)$ on AB can be read off from Fig. 10

$$x(0,\mu)=-r_2+r_2\cos\mu,\ \ y(0,\mu)=r_2\sin\mu\,; \tag{6.13}$$

hence,

$$\begin{aligned}\widetilde{x}(\lambda,\mu)&=-r_2\cos(\lambda-\mu)+r_2\cos\lambda\\ \widetilde{y}(\lambda,\mu)&=r_2\sin(\mu-\lambda)+r_2\sin\lambda.\end{aligned} \tag{6.14}$$

Substitution of (6.7) into (6.11) leads to integral expressions of convolution type, which can be rearranged to the formulae involving Lommel-like functions $F_n(\alpha,\beta)$ (see (a.16)), using the results (A1) and (A2) from the Appendix of the present paper. We find

$$\begin{aligned}\overline{x}(\lambda,\mu)&=r_1F_1(\lambda,\mu)+r_2F_2(\mu,\lambda)\\ \overline{y}(\lambda,\mu)&=r_1F_2(\lambda,\mu)+r_2F_1(\mu,\lambda).\end{aligned} \tag{6.15}$$

The functions above satisfy the differential equations (a.55 and a.56) and are linked with A, B by (a.57). Having found $\overline{x}$, $\overline{y}$ we insert them into (6.10) and invert the latter relations to find

$$\begin{aligned}x(\lambda,\mu)&=\overline{x}(\lambda,\mu)\cos(\mu-\lambda)-\overline{y}(\lambda,\mu)\cdot\sin(\mu-\lambda)\\ y(\lambda,\mu)&=\overline{x}(\lambda,\mu)\sin(\mu-\lambda)+\overline{y}(\lambda,\mu)\cdot\cos(\mu-\lambda).\end{aligned} \tag{6.16}$$

One checks that the functions above satisfy the conditions (6.13) and similar conditions on AC:

$$x(\lambda,0)=r_1\sin\lambda,\qquad y(\lambda,0)=-r_1+r_1\cos\lambda \tag{6.17}$$

(see Fig. 10), where the point $(\lambda,0)$ on the arc AC is shown.

The formula (6.16) makes it possible to write a computer programme generating the Hencky nets for various values of the parameters κ, α_p and β_p, where $(\alpha_p,\ \beta_p)$ are coordinates of point P of application of the force **P**. The coordinates $(\lambda,\ \mu)$ vary within the limits

$$0\le\lambda\le\alpha_p,\qquad 0\le\mu\le\beta_p \tag{6.18}$$

and max $\alpha_p=\theta_1$, max $\beta_p=\theta_2$ (see Fig. 6). Thus, the line BD is a line $\mu=\theta_2$, and the line CD is $\lambda=\theta_1$, where point D has coordinates $(\theta_1,\ \theta_2)$. The formulae derived here hold within the domain BDCA, the geometry of which is known.

A programme written in MAPLE forming the parametric lines $\alpha(\beta=const)$ and $\beta(\alpha=const)$, along with boundary lines BD, CD have made it possible to investigate the shapes of the cantilevers for various values of data κ, α_p, β_p or κ, θ_1, θ_2 (cf. Fig. 11a–d). These figures make it clear that the boundary R_1RNN_1 can be a straight line, and then the whole half-plane is the feasible domain [see Fig. 11c where $\alpha_p=\beta_p=(3/4)\pi$]. The feasible domain can encompass three quarters of the plane [see Fig. 11d for $\alpha_p=(7/4)\pi$, $\beta_p=\pi/5$].

Remark. In case of $\kappa=1$ we have $r_1=r_2$ and then

$$A(\alpha,\beta)=B(\beta,\alpha),\ x(\alpha,\beta)=y(\beta,\alpha)\,. \tag{6.19}$$

7 Chan-like designs of first rank

We consider position of point P outside the domain BDCA in the regions CDG and BDH adjacent to the bounding lines

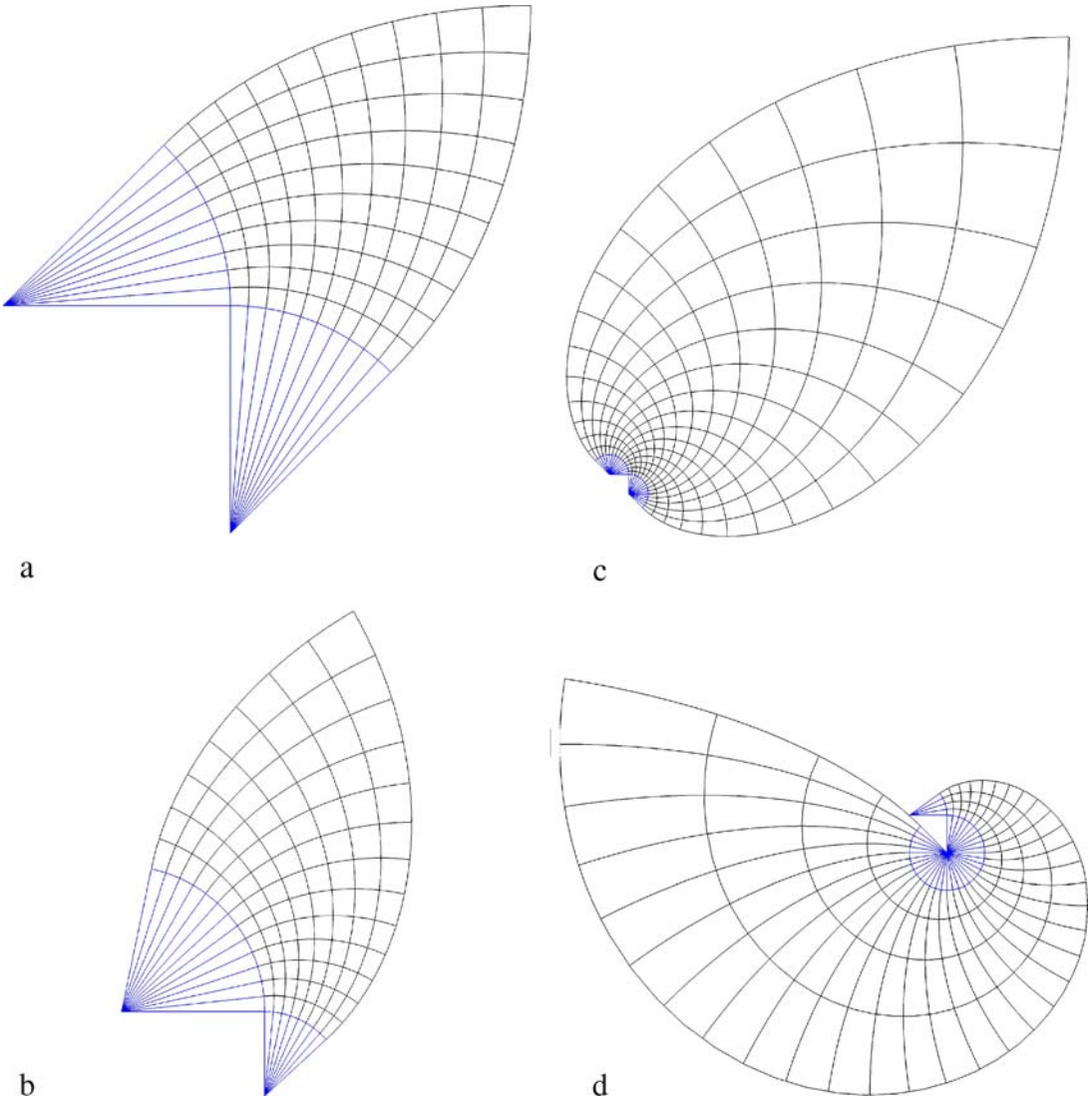

Fig. 11 **a** Michell cantilever, $\kappa = 1$, $\alpha_p = \frac{\pi}{4}$, $\beta_p = \frac{\pi}{4}$. **b** Michell cantilever, $\kappa = 3$, $\alpha_p = \frac{4\pi}{15}$, $\beta_p = \frac{13\pi}{30}$. **c** Michell cantilever, $\kappa = 1$, $\alpha_p = \frac{3\pi}{4}$, $\beta_p = \frac{3\pi}{4}$. **d** Michell cantilever, $\kappa = 1$, $\alpha_p = \frac{7\pi}{4}$, $\beta_p = \frac{\pi}{5}$

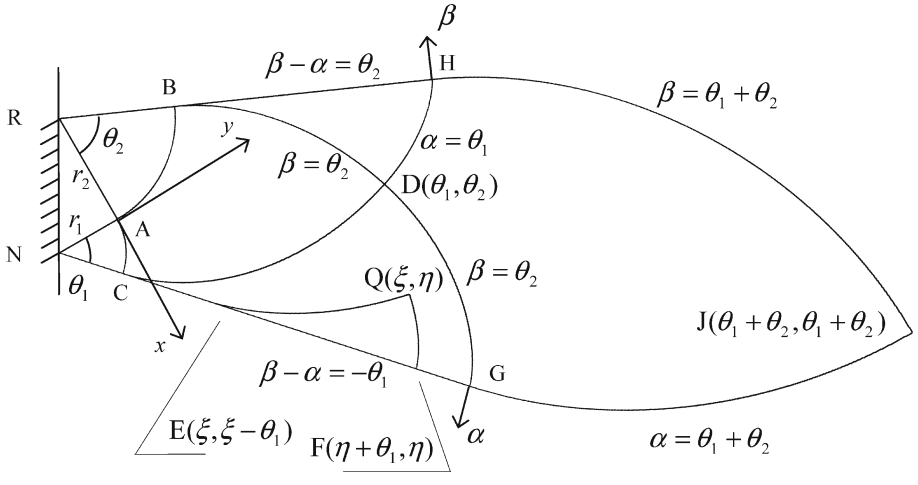

Fig. 12 Chan-like problem

NN_1, RR_1 (see Fig. 12). Determination of Cartesian coordinates $x(\alpha,\beta)$, $y(\alpha,\beta)$ of points of parametric lines and the fields $A(\alpha,\beta)$, $B(\alpha,\beta)$ within the domains BDH and CDG is much more complicated than in the previous subdomains. Now we cannot make use directly of Riemann's formula (a.17) with reference neither to the functions $A(\alpha,\beta)$, $B(\alpha,\beta)$ nor to the functions $\overline{x}(\alpha,\beta)$, $\overline{y}(\alpha,\beta)$ [although all these functions satisfy the hyperbolic equation $Lf=0$, see (6.3)] because the lines CG and BH are not characteristic lines.

An effective method of finding the fields $A(\alpha,\beta)$, $B(\alpha,\beta)$, $\overline{x}(\alpha,\beta)$, $\overline{y}(\alpha,\beta)$ was ingeniously put forward by Chan (1967) for the case of $\kappa=1$ by reducing the problem to one Volterra-type integral equation of convolution form and then by solving this integral equation by the Laplace transform technique. We show below that the method of Chan can be applied also in the case of $\kappa\neq1$ to find the fields $A(\alpha,\beta)$, $B(\alpha,\beta)$, $\overline{x}(\alpha,\beta)$, $\overline{y}(\alpha,\beta)$ and also $x(\alpha,\beta)$, $y(\alpha,\beta)$ in the domains CDG, BDH. This generalization is the subject of this section. The curvilinear coordinates of points G and H are $(\theta_1+\theta_2, \theta_2)$ and $(\theta_1, \theta_1+\theta_2)$, respectively.

7.1 Domain CDG

The function $\overline{x}(\alpha,\beta)$ will be the main unknown. Having this field one can find $\overline{y}(\alpha,\beta)=\partial\overline{x}(\alpha,\beta)\big/\partial\beta$ and then A and B by (a.57). The function $\overline{x}(\alpha,\beta)$ is continuous; hence, its values along CD, where $\alpha=\theta_1$, are given by $(6.15)_1$

$$\overline{x}(\theta_1,\beta)=r_1F_1(\theta_1,\beta)+r_2F_2(\beta,\theta_1). \tag{7.1}$$

On the other hand, we know the equation of the boundary line CG

$$x\cdot\cos\theta_1-y\cdot\sin\theta_1=r_1\sin\theta_1, \tag{7.2}$$

which can be rewritten in the form

$$[x(\alpha,\beta)\cos(\beta-\alpha)+y(\alpha,\beta)\sin(\beta-\alpha)]_{|\beta-\alpha=-\theta_1} = r_1\cdot\sin\theta_1. \tag{7.3}$$

Note that $\beta-\alpha=-\theta_1$ along CG. By (6.10) the equation (7.3) can be expressed in terms of $\overline{x}(\alpha,\beta)$

$$\overline{x}(\alpha,\beta)_{|\beta-\alpha=-\theta_1}=r_1\cdot\sin\theta_1 \tag{7.4}$$

and becomes the boundary condition of the problem. Note that $\overline{x}=$const along CG. Following Chan (1967) we use the Riemann method and apply it to the domain EQF. Thus, we find the representation of the unknown function

$$\overline{x}(\xi,\eta)=r_1\sin\theta_1\cos(\eta+\theta_1-\xi) -\frac{1}{2}\int_{\xi}^{\eta+\theta_1}D_0(\alpha-\xi,\eta+\theta_1-\alpha)\varphi(\alpha)d\alpha, \tag{7.5}$$

where

$$\varphi(\alpha)=\left(\frac{\partial\overline{x}}{\partial\alpha}-\frac{\partial\overline{x}}{\partial\beta}\right)_{\beta=\alpha-\theta_1} \tag{7.6}$$

and

$$D_0(\alpha,\beta)=J_0\Big(2(\alpha\beta)^{1/2}\Big), \tag{7.7}$$

where J_0 is Bessel function of first kind of order zero. The details of the derivation of (7.5) can be found in Appendix B. Function $\varphi(a)$ has nothing to do with angle φ in Fig. 1.

The integration domain is shown in Fig. 13. It is visible that both the arguments of D_0 in (7.5) are nonnegative. By (6.15) we have (7.1), and by using the identity (a.11) we write

$$\overline{x}(\theta_1,\beta)=r_1F_1(\beta,\theta_1)+r_2F_2(\beta,\theta_1)-r_1\sin(\beta-\theta_1). \tag{7.9}$$

Thus, the property of continuity of $\overline{x}$ along the line $\alpha=\theta_1$ or the line CD gives the following integral equation for $\varphi(a)$

$$\int_{\theta_1}^{\eta+\theta_1}D_0(\alpha-\theta_1,\eta+\theta_1-\alpha)\varphi(\alpha)d\alpha = -2[r_1F_1(\eta,\theta_1)+r_2F_2(\eta,\theta_1)-r_1\cdot\sin(\eta-\theta_1)-r_1\cos\eta\sin\theta_1]. \tag{7.10}$$

This integral equation can be solved by the method of Chan (1967). We introduce a new function $\overline{\varphi}(\alpha)$ such that $\varphi(\alpha)=\overline{\varphi}(\alpha-\theta_1)$ and rearrange the l.h.s. of (7.10) to the convolution form

$$\int_0^{\eta}D_0(x,\eta-x)\overline{\varphi}(x)dx = -2[r_1F_1(\eta,\theta_1)+r_2F_2(\eta,\theta_1)-r_1\cos\theta_1\sin\eta]. \tag{7.11}$$

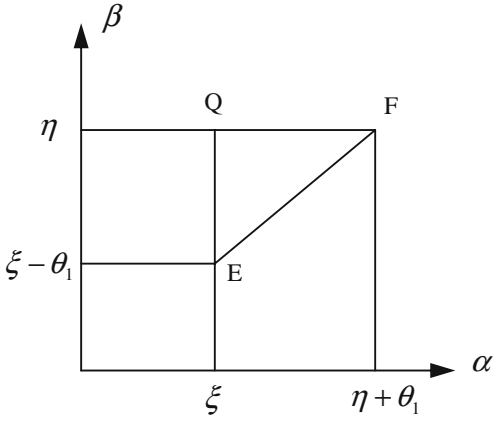

Fig. 13 Triangle of integration

Now this integral equation can be solved by applying the Laplace transform L_η to both sides of (7.11). We use notation (a.25) and the results (a.174) and (a.29) to find

$$\frac{1}{p}\overline{\varphi}^*\left(p+\frac{1}{p}\right) = -2\left\{r_1\frac{\exp\left(\theta_1/p\right)}{p^2+1}+r_2\frac{\exp\left(\theta_1/p\right)}{p\left(p^2+1\right)}-r_1\frac{\cos\theta_1}{p^2+1}\right\}. \tag{7.12}$$

We change the variable p into s:

$$p+\frac{1}{p}=s;\quad p=\frac{1}{2}(s+R);\quad R=\sqrt{s^2-4};$$
$$\frac{1}{p}=\frac{2}{s+R},\quad \frac{1}{p}=\frac{1}{2}(s-R),\quad \frac{p}{p^2+1}=\frac{1}{s} \tag{7.13}$$

and rearrange (7.12) to the form

$$\overline{\varphi}^*(s) = -2\left[\frac{\exp\left[\frac{1}{2}\theta_1\{s-R\}\right]}{R}\left\{r_2\cdot\frac{2}{s}-r_1\frac{4}{s(s+R)}+r_1-r_2\cdot\frac{2}{s+R}\right\}-r_1\cdot\frac{\cos\theta_1}{s}\right]. \tag{7.14}$$

By taking advantage of the Laplace transforms (a.164) and (a.165) we find

$$\overline{\varphi}(x) = -2[2r_2F_1(x,x+\theta_1)-2r_1F_2(x,x+\theta_1) + r_1G_0(x,x+\theta_1)-r_2G_1(x,x+\theta_1)-r_1\cos\theta_1]$$

and come back to the unknown φ

$$\varphi(\alpha) = -2[2r_2F_1(\alpha-\theta_1,\alpha)-2r_1F_2(\alpha-\theta_1,\alpha) + r_1G_0(\alpha-\theta_1,\alpha)-r_2G_1(\alpha-\theta_1,\alpha)-r_1\cos\theta_1]. \tag{7.15}$$

Thus, (7.10) has been solved. The formula (7.15) should now be put into (7.5). The integrals which appear can be calculated and expressed in terms of Lommel-like functions $F_n(\alpha,\beta)$. Indeed, we find the following expression for $\overline{x}$

$$\begin{aligned}\overline{x}(\xi,\eta) = {} & r_1\sin\theta_1\cos(\eta+\theta_1-\xi)-r_1\cos\theta_1\int_\xi^{\eta+\theta_1}D_0(\alpha-\xi,\eta+\theta_1-\alpha)d\alpha\\ & +r_2\int_\xi^{\eta+\theta_1}D_0(\alpha-\xi,\eta+\theta_1-\alpha)[2F_1(\alpha-\theta_1,\alpha)-G_1(\alpha-\theta_1,\alpha)]d\alpha\\ & +r_1\int_\xi^{\eta+\theta_1}D_0(\alpha-\xi,\eta+\theta_1-\alpha)[2F_0(\alpha-\theta_1,\alpha)-G_0(\alpha-\theta_1,\alpha)]d\alpha,\end{aligned} \tag{7.16a}$$

where the identity $2F_2-G_0=-(2F_0-G_0)$ has been used (see (a.7)). Now we rearrange (7.16a). By using (A3) we compute

$$\int_\xi^{\eta+\theta_1}D_0(\alpha-\xi,\eta+\theta_1-\alpha)d\alpha = \int_0^{\eta+\theta_1-\xi}D_0(\alpha_1,\eta+\theta_1-\alpha_1)d\alpha_1 = \sin(\eta+\theta_1-\xi) \tag{7.16b}$$

and write (7.16a) in the form

$$\overline{x}(\xi,\eta) = r_1\sin(\xi-\eta)+r_2\left[J_1^L-J_1^P\right]+r_1\left[J_0^L-J_0^P\right] \tag{7.16c}$$

with

$$J_n^L = \int_{\theta_1}^{\eta+\theta_1}D_0(\alpha-\xi,\eta+\theta_1-\alpha)\left[2F_n(\alpha-\theta_1,\alpha)-G_n(\alpha-\theta_1,\alpha)\right]d\alpha$$
$$J_n^P = \int_{\theta_1}^{\xi}D_0(\alpha-\xi,\eta+\theta_1-\alpha)\left[2F_n(\alpha-\theta_1,\alpha)-G_n(\alpha-\theta_1,\alpha)\right]d\alpha. \tag{7.16d}$$

We express the above integrals by using the notation in (b.166)–(b.168) and (b.176):

$$J_n^L = w_n(-\theta_1+\xi,-\theta_1;\eta),\quad J_n^P = w_n(\eta,-\theta_1;-\theta_1+\xi) \tag{7.16e}$$

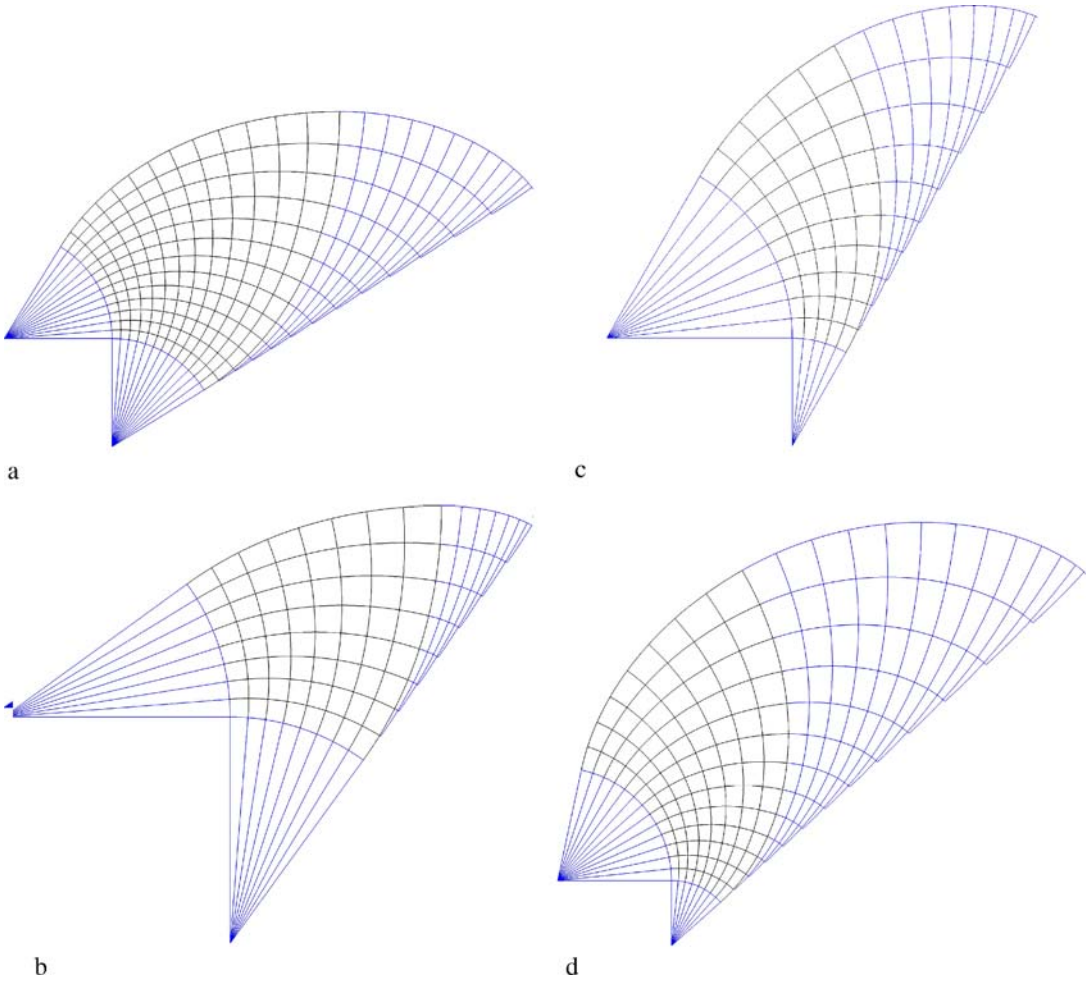

Fig. 14 **a** Michell cantilever, $\kappa = 1,\ \theta_1 = \frac{13\pi}{40},\ \alpha_p = \frac{13\pi}{20},\ \beta_p = \frac{13\pi}{40}$. **b** Michell cantilever, $\kappa = 1,\ \theta_1 = \frac{\pi}{5},\ \alpha_p = \frac{2\pi}{5},\ \beta_p = \frac{\pi}{5}$. **c** Michell cantilever, $\kappa = 3,\ \theta_1 = \frac{\pi}{6},\ \alpha_p = \frac{\pi}{2},\ \beta_p = \frac{\pi}{3}$. **d** Michell cantilever, $\kappa = 3,\ \theta_1 = \frac{4\pi}{15},\ \alpha_p = \frac{7\pi}{10},\ \beta_p = \frac{13\pi}{30}$

and using the results (b.172) we find

$$J_n^L = F_{n+1}(\eta, \xi), \quad J_n^P = F_{n+1}(\xi - \theta_1, \eta + \theta_1)\,. \tag{7.16f}$$

Substitution of (7.16f) into (7.16c) gives

$$\begin{aligned}\overline{x}(\xi, \eta) = {} & r_1[F_1(\eta, \xi) - F_1(\xi - \theta_1, \eta + \theta_1)] \\ & + r_2[F_2(\eta, \xi) - F_2(\xi - \theta_1, \eta + \theta_1)] \\ & - r_1 \sin(\eta - \xi).\end{aligned} \tag{7.17}$$

By using (a.11) we rearrange the above formula as follows:

$$\begin{aligned}\overline{x}(\xi, \eta) = {} & r_1[F_1(\xi, \eta) - F_1(\xi - \theta_1, \eta + \theta_1)] \\ & + r_2[F_2(\eta, \xi) - F_2(\xi - \theta_1, \eta + \theta_1)].\end{aligned} \tag{7.18}$$

The equation $\frac{\partial \overline{x}(\alpha,\beta)}{\partial \beta} = \overline{y}(\alpha, \beta)$ along with the differentiation rules (a.4) give

$$\begin{aligned}\overline{y}(\xi, \eta) = {} & r_1[F_2(\xi, \eta) - F_2(\xi - \theta_1, \eta + \theta_1)] \\ & + r_2[F_1(\eta, \xi) - F_3(\xi - \theta_1, \eta + \theta_1)].\end{aligned} \tag{7.19}$$

The coordinates x,y should be then expressed by (6.16). The functions $\overline{x}$, $\overline{y}$, x, y are continuous in the domain CABDGC; they do not suffer jumps along CD.

Having found $\overline{x}$, $\overline{y}$ one can compute A,B by (a.57) with using (a.4), which gives

$$\begin{aligned}A(\alpha, \beta) = {} & r_1[G_0(\alpha, \beta) - G_0(\alpha - \theta_1, \beta + \theta_1)] \\ & + r_2[G_1(\beta, \alpha) - G_1(\alpha - \theta_1, \beta + \theta_1)] \\ B(\alpha, \beta) = {} & r_1[G_1(\alpha, \beta) - G_1(\alpha - \theta_1, \beta + \theta_1)] \\ & + r_2[G_0(\beta, \alpha) - G_2(\alpha - \theta_1, \beta + \theta_1)].\end{aligned} \tag{7.20}$$

We note that B is continuous along CD, while A suffers a jump:

$$[\![A]\!]_{CD} = A_{|CDG}(\theta_1, \beta) - A_{|ABDC}(\theta_1, \beta)$$

equal to

$$[\![A]\!]_{CD} = -r_1(\theta_1 + \beta). \tag{7.21}$$

Let us compute now A along CG, where $\beta{=}\alpha{-}\theta_1$. According to (7.20) we find

$$A(\alpha, \alpha - \theta_1) = 0, \tag{7.22}$$

which means that β lines are tangent to CG.

Remark 7.1. The formulae (7.18) and (7.19) can be predicted by the following mnemonic method. We write $\overline{x}$ along CG by using (6.15):

$$\overline{x}(\alpha, \alpha - \theta_1) = r_1 F_1(\alpha, \alpha - \theta_1) + r_2 F_2(\alpha - \theta_1, \alpha) + \Delta\overline{x}(\alpha, \alpha - \theta_1). \tag{7.23}$$

By recalling (7.4) we find

$$\Delta\overline{x}(\alpha, \alpha - \theta_1) = r_1 \sin\theta_1 - r_1 F_1(\alpha, \alpha - \theta_1) - r_2 F_2(\alpha - \theta_1, \alpha),$$

and by using (a.11), we write

$$\Delta\overline{x}(\alpha, \alpha - \theta_1) = -r_1 F_1(\alpha - \theta_1, \alpha) - r_2 F_2(\alpha - \theta_1, \alpha). \tag{7.24}$$

We postulate the following extrapolation of $\Delta\overline{x}$ into the domain CDG:

$$\Delta\overline{x}^{CDG}(\alpha, \beta) = -r_1 F_1(\alpha - \theta_1, \beta + \theta_1) - r_2 F_2(\alpha - \theta_1, \beta + \theta_1), \tag{7.25}$$

where the second argument $\alpha{-}\theta_1$ has been replaced by β. Thus, we write

$$\overline{x}(\alpha, \beta) = \underbrace{r_1 F_1(\alpha, \beta) + r_2 F_2(\beta, \alpha)}_{ABDC} + \Delta\overline{x}^{CDG}(\alpha, \beta) \tag{7.26}$$

and arrive at (7.18).

Now we can construct some exemplary nets for selected values of $\kappa, \theta_1, \theta_2, \alpha_p, \beta_p$ (see Fig. 14a–d). Angle θ_2 satisfies the condition $\theta_2 \geq \beta_p$.

7.2 Domain BDH

Now the function $\overline{y}(\alpha, \beta)$ is our main unknown. According to (6.15), due to continuity, this function along the BD line has the form

$$\overline{y}(\alpha, \theta_2) = r_2 F_1(\theta_2, \alpha) + r_1 F_2(\alpha, \theta_2),$$

or, by (a.11), we have

$$\overline{y}(\alpha, \theta_2) = r_2 F_1(\alpha, \theta_2) + r_1 F_2(\alpha, \theta_2) - r_2 \sin(\alpha - \theta_2). \tag{7.27}$$

The equation

$$-x \cdot \sin\theta_2 + y \cdot \cos\theta_2 = r_2 \sin\theta_2 \tag{7.28}$$

of the line BH (see Fig. 12) can be put in terms of $\overline{y}$ [see (6.10)] by

$$\overline{y}_{|\beta-\alpha=\theta_2} = r_2 \sin\theta_2. \tag{7.29}$$

Let us note analogies between the formulae (7.27), (7.29) and (7.9), (7.4). Substitution

$$\beta \mapsto \alpha, \quad \theta_1 \mapsto \theta_2, \quad r_1 \mapsto r_2, \quad \overline{x} \mapsto \overline{y}$$

changes the latter equations into the former. We should repeat the derivation for the curvilinear triangle BDH with using

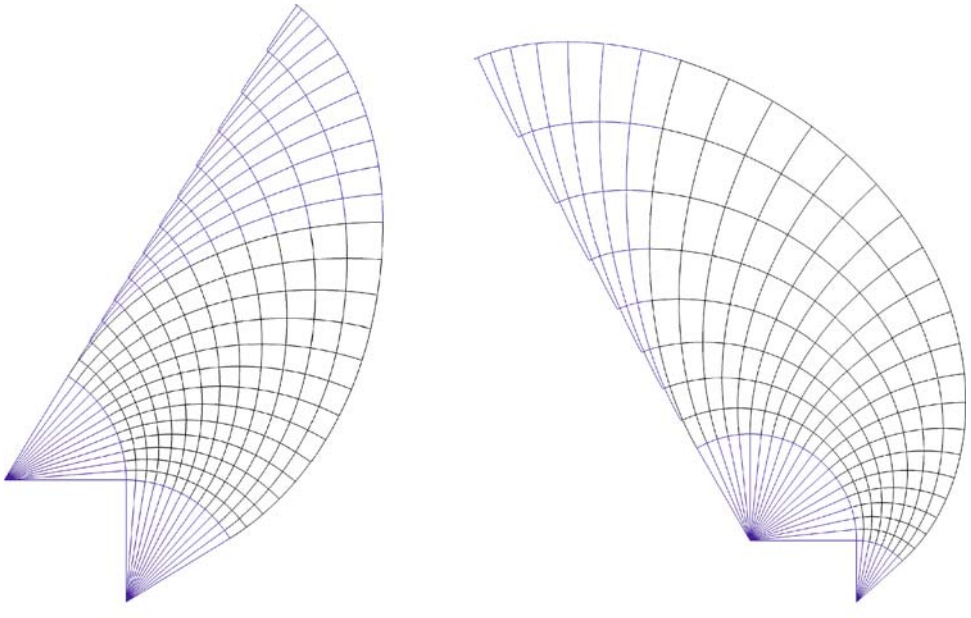

a b

Fig. 15 **a** Michell cantilever, $\kappa = 1$, $\theta_2 = \frac{13\pi}{40}$, $\alpha_p = \frac{13\pi}{40}$, $\beta_p = \frac{13\pi}{20}$. **b** Michell cantilever, $\kappa = 3$, $\theta_2 = \frac{2\pi}{3}$, $\alpha_p = \frac{4\pi}{15}$, $\beta_p = \frac{14\pi}{15}$

analogies above. Thus, we arrive at the counterparts of the formulae (7.18) and (7.19):

$$\begin{aligned}\overline{y}(\alpha,\beta) &= r_2F_1(\beta,\alpha)+r_1F_2(\alpha,\beta)-r_2F_1(\beta-\theta_2,\alpha+\theta_2)\\ &\quad -r_1F_2(\beta-\theta_2,\alpha+\theta_2)\\ \overline{x}(\alpha,\beta) &= r_2F_2(\beta,\alpha)+r_1F_1(\alpha,\beta)-r_2F_2(\beta-\theta_2,\alpha+\theta_2)\\ &\quad -r_1F_3(\beta-\theta_2,\alpha+\theta_2)\end{aligned}\tag{7.30}$$

and find the Lamé fields

$$\begin{aligned}A(\alpha,\beta) &= r_2G_1(\beta,\alpha)+r_1G_0(\alpha,\beta)-r_2G_1(\beta-\theta_2,\alpha+\theta_2)\\ &\quad -r_1G_2(\beta-\theta_2,\alpha+\theta_2)\\ B(\alpha,\beta) &= r_2G_0(\beta,\alpha)+r_1G_1(\alpha,\beta)-r_2G_0(\beta-\theta_2,\alpha+\theta_2)\\ &\quad -r_1G_1(\beta-\theta_2,\alpha+\theta_2).\end{aligned}\tag{7.31}$$

The function A is continuous along BD, while B suffers there a jump

$$[\![B]\!]_{BD} = B_{|BDH}(\alpha,\theta_2)-B_{|ABDC}(\alpha,\theta_2)\tag{7.32}$$

$$[\![B]\!]_{BD} = r_2(\theta_2+\alpha).\tag{7.33}$$

Along the line BH, where $\beta-\alpha=\theta_2$, we have $B(\alpha,\alpha+\theta_2)=0$. Thus, the α lines are tangent to BH.

In case of $\kappa=1$ $r_1=r_2$, $\theta_1=\theta_2$, the domains CDG and BDH are mutually symmetric with respect to the AD line. The formulae for x, y, A, B found here coincide with appropriate formulae of Section a.6.

Some extensions to the BDH domain are shown in Fig. 15. Angle θ_1 satisfies the condition $\theta_1\geq\alpha_p$.

8 Hencky net in DHJG domain

For the case of $\kappa=1$ this net has been constructed in Lewiński et al. (1994a) by using the Riemann method, taking advantage of continuity of $\overline{x}$ and $\overline{y}$ along the lines DH and DG. This method can also be used for the case of $\kappa\neq1$. To save space we shall not derive the net but guess it by applying the reasoning similar to that explained in Remark 7.1.

The field $\overline{x}$ within CDG can be decomposed as in Remark 7.1 see (7.26)

$$\overline{x}_{|CDG} = \overline{x}^{ABDC}+\Delta\overline{x}^{CDG},\tag{8.1}$$

and similarly for BDH

$$\overline{x}_{|BDH} = \overline{x}^{ABDC}+\Delta\overline{x}^{BDH}.\tag{8.2}$$

The notation $\overline{x}^{ABDC}$ means extension of the function (6.15) into the whole feasible domain. We note that $\Delta\overline{x}^{CDG}$ vanishes on the line CD and on its extension DH. Similarly, $\Delta\overline{x}^{BDH}$ vanishes on BD and on its extension DG. Let us construct

$$\overline{x} = \overline{x}^{ABDC}+\Delta\overline{x}^{CDG}+\Delta\overline{x}^{BDH}.\tag{8.3}$$

The field $\overline{x}$ constructed as above satisfies the boundary conditions along DG and DH. Moreover, $\overline{x}$ defined by (8.3) satisfies the governing equation $L\overline{x}=0$ because all its components satisfy this equation. Let us write down this formula explicitly:

$$\overline{x}(\alpha,\beta)=\overbrace{r_1F_1(\alpha,\beta)+r_2F_2(\beta,\alpha)}^{ABDC}-\overbrace{r_1F_1(\alpha-\theta_1,\beta+\theta_1)-r_2F_2(\alpha-\theta_1,\beta+\theta_1)}^{CDG}\underbrace{-r_2F_2(\beta-\theta_2,\alpha+\theta_2)-r_1F_3(\beta-\theta_2,\alpha+\theta_2)}_{BDH},\tag{8.4}$$

with subsequent components corresponding to the decomposition (8.3). By arguments invoked above the expression (8.4) satisfies all necessary conditions; hence, $\overline{x}$ given by (8.4) is really the solution to our problem. Appropriate differentiation gives the field $\overline{y}$

$$\overline{y}(\alpha,\beta)=\overbrace{r_1F_2(\alpha,\beta)+r_2F_1(\beta,\alpha)}^{ABDC}-\overbrace{r_1F_2(\alpha-\theta_1,\beta+\theta_1)-r_2F_3(\alpha-\theta_1,\beta+\theta_1)}^{CDG}\underbrace{-r_2F_1(\beta-\theta_2,\alpha+\theta_2)-r_1F_2(\beta-\theta_2,\alpha+\theta_2)}_{BDH}.\tag{8.5}$$

Now we can find the Lamé coefficients by (a.57):

$$\begin{aligned}A(\alpha,\beta) &= r_1G_0(\alpha,\beta)+r_2G_1(\beta,\alpha)-r_1G_0(\alpha-\theta_1,\beta+\theta_1)\\ &\quad -r_2G_1(\alpha-\theta_1,\beta+\theta_1)-r_2G_1(\beta-\theta_2,\alpha+\theta_2)\\ &\quad -r_1G_2(\beta-\theta_2,\alpha+\theta_2)\\ B(\alpha,\beta) &= r_1G_1(\alpha,\beta)+r_2G_0(\alpha,\beta)-r_1G_1(\alpha-\theta_1,\beta+\theta_1)\\ &\quad -r_2G_2(\alpha-\theta_1,\beta+\theta_1)-r_2G_0(\beta-\theta_2,\alpha+\theta_2)\\ &\quad -r_1G_1(\beta-\theta_2,\alpha+\theta_2).\end{aligned}\tag{8.6}$$

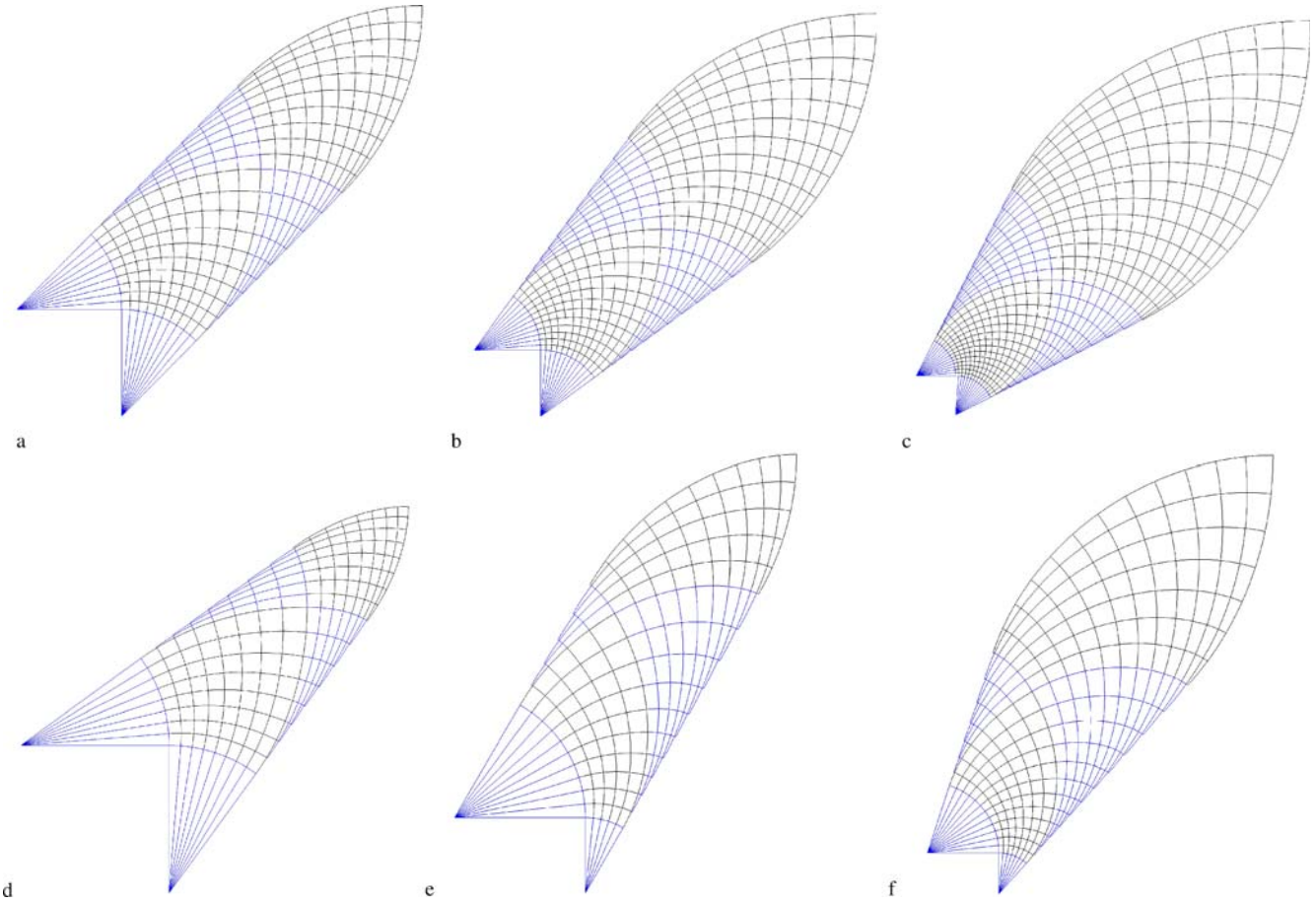

Fig. 16 **a** Michell cantilever, $\kappa = 1$, $\theta_1 = \frac{\pi}{4}$, $\theta_2 = \frac{\pi}{4}$, $\alpha_p = \frac{\pi}{2}$, $\beta_p = \frac{\pi}{2}$. **b** Michell cantilever, $\kappa = 1$, $\theta_1 = \frac{3\pi}{10}$, $\theta_2 = \frac{3\pi}{10}$, $\alpha_p = \frac{3\pi}{5}$, $\beta_p = \frac{3\pi}{5}$. **c** Michell cantilever, $\kappa = 1$, $\theta_1 = \frac{7\pi}{20}$, $\theta_2 = \frac{7\pi}{20}$, $\alpha_p = \frac{7\pi}{10}$, $\beta_p = \frac{7\pi}{10}$. **d** Michell cantilever, $\kappa = 1$, $\theta_1 = \frac{\pi}{5}$, $\theta_2 = \frac{\pi}{5}$, $\alpha_p = \frac{2\pi}{5}$, $\beta_p = \frac{2\pi}{5}$. **e** Michell cantilever, $\kappa = 3$, $\theta_1 = \frac{\pi}{6}$, $\theta_2 = \frac{2\pi}{6}$, $\alpha_p = \frac{\pi}{2}$, $\beta_p = \frac{\pi}{2}$. **f** Michell cantilever, $\kappa = 3$, $\theta_1 = \frac{7\pi}{30}$, $\theta_2 = \frac{2\pi}{5}$, $\alpha_p = \frac{19\pi}{30}$, $\beta_p = \frac{19\pi}{30}$.

For the case of κ=1, r_1=r_2 and θ_1= θ_2, the formulae (8.4)–(8.6) coincide with appropriate formulae of Section a.7.

Let us observe that the function A is constructed from $\overline{x}$ by replacing F with G and decreasing the indices by 1. In a similar manner one can construct B from $\overline{y}$. This mnemonic rule should not be used in the opposite direction because $G_0(\alpha,0)$=$G_0(0,\alpha)$; $F_0(\alpha,0)\neq F_0(0,\alpha)$.

In the case of $\kappa = 1$, $\theta_1 = \theta_2 = \pi/4$, the feasible domain is a strip; BH and CG lines are parallel (see Fig. 16a).

For θ_1=θ_2=3π/10 (see Fig. 16b) and θ_1=θ_2=7π/20 (Fig. 16c), the domain DHJG becomes larger and larger.

The results found above hold good even if the lines RB and NC intersect in the feasible domain Ω (see Fig. 16d) for κ=1. The case of RB parallel to NC and κ=3 is shown in Fig. 16e. One notes that the domains BDH and CDG cease to be equal if $\kappa\neq 1$.

The lines BA, AC, BDG, CDH will be called lines of geometric division. They are discontinuity lines of A or B fields, as can be seen in Fig. 17a,b, for $\kappa = 1$, $\theta_1 = \theta_2 = 13\pi/40$ and in Fig. 18a,b for $\kappa = 3$, $\theta_1 = \pi/6$, $\theta_2 = \pi/3$.

9 Chan-like designs of second rank

If the loading is applied at a point within Ω_0 but outside the region RHJGCNR the Hencky net constructions of the previous sections are not sufficient. The net should be extended through the lines HJ and JG to construct the Chan-like domains GJG_2 and HJH_2 and then to find the Hencky net within $JH_2J_2G_2$ (see Fig. 19).

The curvilinear coordinates of points G_2, H_2, J_2 are $(2\theta_1+\theta_2,\theta_1+\theta_2)$, $(\theta_1+\theta_2, \theta_1+2\theta_2)$, $(2\theta_1+\theta_2, \theta_1+2\theta_2)$. Finding geometric characteristics of the domain GJG_2 is fairly complicated because similarly as in the case of Chan domains of the first kind, we cannot apply directly the Riemann formula

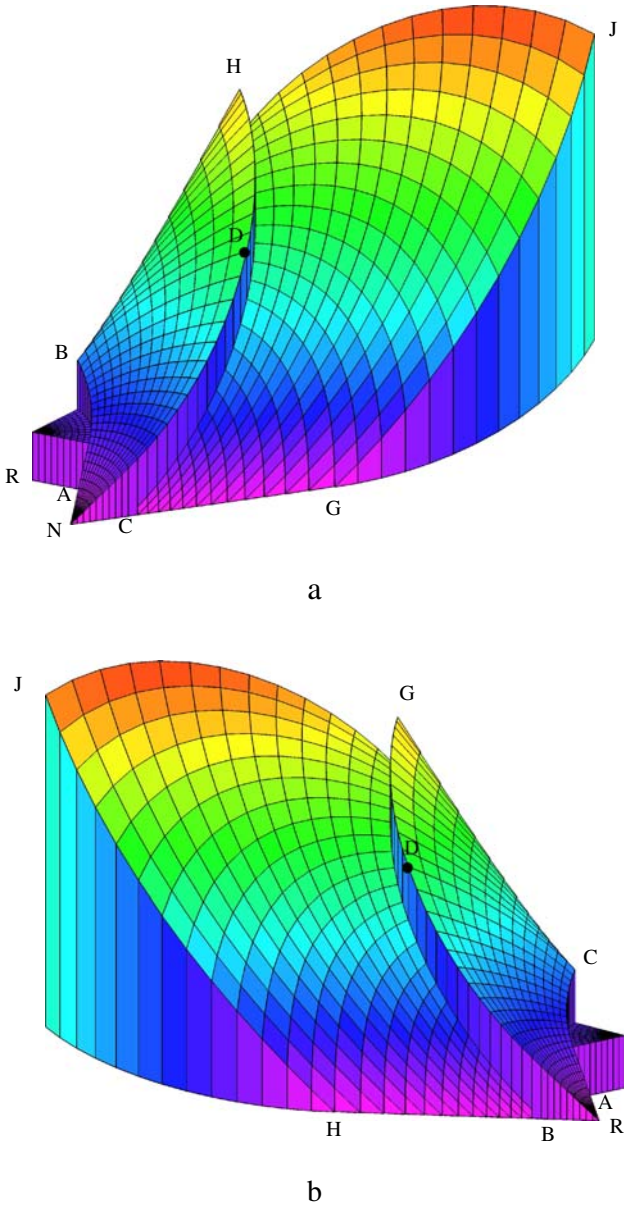

Fig. 17 **a** Lamé field $A(\alpha,\beta)$, $\kappa = 1$, $\theta_1 = \theta_2 = \frac{13\pi}{40}$. **b** Lamé field $B(\alpha,\beta)$, $\kappa = 1$, $\theta_1 = \theta_2 = \frac{13\pi}{40}$

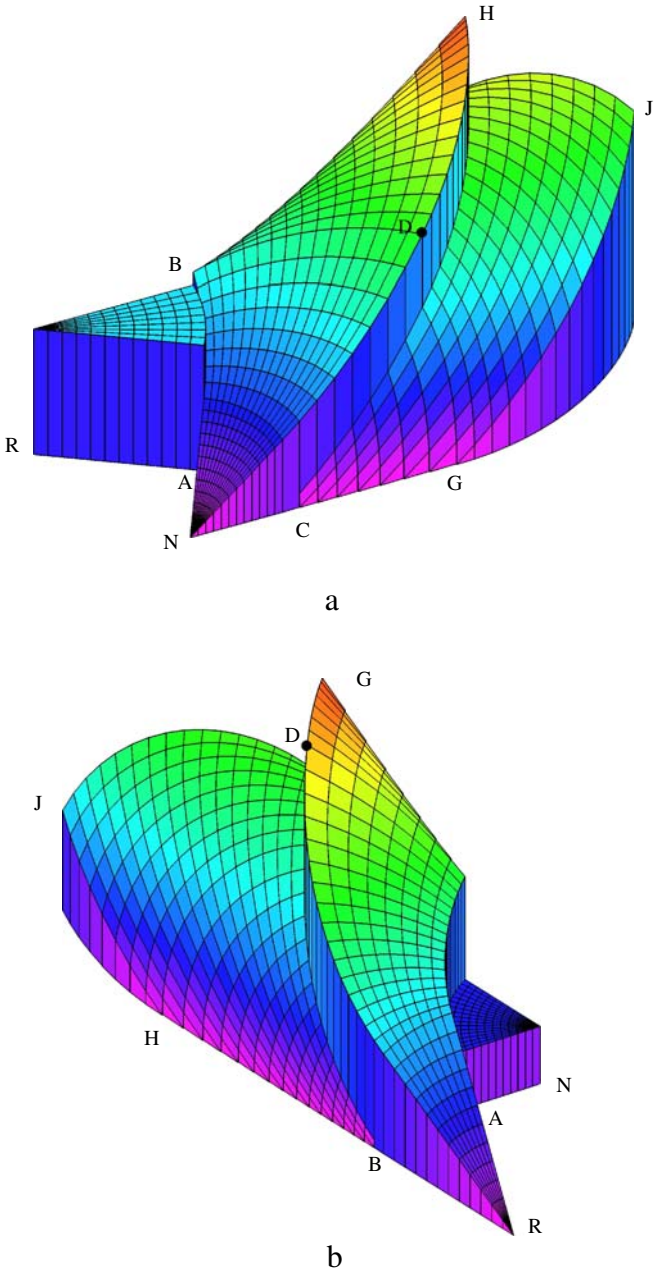

Fig. 18 **a** Lamé field $A(\alpha,\beta)$, $\kappa = 3$, $\theta_1 = \frac{\pi}{6}$, $\theta_2 = \frac{\pi}{3}$. **b** Lamé field $B(\alpha,\beta)$, $\kappa = 3$, $\theta_1 = \frac{\pi}{6}$, $\theta_2 = \frac{\pi}{3}$

for any of the unknown functions. Indeed, the lines GG_2 and HH_2 are not characteristic lines. Moreover, the function $\overline{x}$ in domain DHJG has a more complicated form than in the region ABDC. It occurs, however, that we can omit the difficulties because the result can be similarly guessed, as has been shown in Remark 7.1. To find the solution we write the values of function $\overline{x}$ on the straight boundary GG_2

$$\begin{aligned}\overline{x}(\alpha, \alpha-\theta_1) &= \overline{x}^{ABDC}(\alpha, \alpha-\theta_1) + \Delta\overline{x}^{CDG}(\alpha, \alpha-\theta_1)\\ &\quad + \Delta\overline{x}^{BDH}(\alpha, \alpha-\theta_1) + \Delta\overline{x}^{GJG_2}(\alpha, \alpha-\theta_1)\\ &= r_1 \sin\theta_1. \end{aligned} \tag{9.1}$$

Along the straight edge CG the following equality holds:

$$\begin{aligned}\overline{x}^{CDG}(\alpha, \alpha-\theta_1) &= \overline{x}^{ABDC}(\alpha, \alpha-\theta_1) + \Delta x^{CDG}(\alpha, \alpha-\theta_1)\\ &= r_1 \sin\theta_1, \end{aligned} \tag{9.2}$$

and consequently, the following equation is true:

$$\Delta\overline{x}^{BDH}(\alpha, \alpha-\theta_1) + \Delta\overline{x}^{GJG_2}(\alpha, \alpha-\theta_1) = 0. \tag{9.3}$$

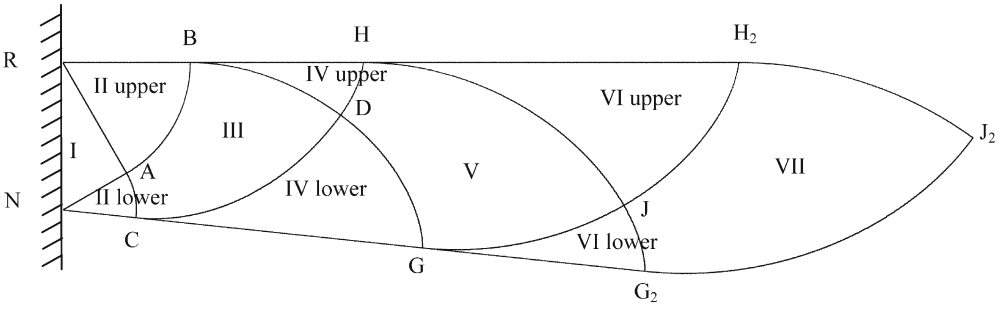

Fig. 19 Chan-like structures of second rank

In this manner we find the values of function $\Delta\overline{x}^{GJG_2}$ along the line GG_2

$$\Delta\overline{x}^{GJG_2}(\alpha,\alpha-\theta_1)=r_2F_2(\alpha-(\theta_1+\theta_2),\alpha+\theta_2) -r_1F_3(\alpha-(\theta_1+\theta_2),\alpha+\theta_2). \quad (9.4)$$

Now we postulate the following extrapolation of function $\Delta\overline{x}$ into the domain GJG_2:

$$\Delta\overline{x}^{GJG_2}(\alpha,\beta)=r_2F_2(\alpha-(\theta_1+\theta_2),\beta+(\theta_1+\theta_2)) +r_1F_3(\alpha-(\theta_1+\theta_2),\beta+(\theta_1+\theta_2)), \quad (9.5)$$

where the second argument of $\Delta\overline{x}^{GJG_2}$ or $\alpha-\theta_1$ has been replaced by β. Eventually, the coordinates $\overline{x}(\alpha,\beta)$, $\overline{y}(\alpha,\beta)$ in the domain GJG_2 are expressed by Lommel functions as follows:

$$\begin{aligned}\overline{x}(\xi,\eta)&=r_1F_1(\xi,\eta)+r_2F_2(\eta,\xi)-r_1F_1(\xi-\theta_1,\eta+\theta_1)\\&-r_2F_2(\xi-\theta_1,\eta+\theta_1)-r_2F_2(\eta-\theta_2,\xi+\theta_2)\\&-r_1F_3(\eta-\theta_2,\xi+\theta_2)\\&+r_2F_2(\xi-\theta_1-\theta_2,\eta+\theta_1+\theta_2)\\&+r_1F_3(\xi-\theta_1-\theta_2,\eta+\theta_1+\theta_2) \quad (9.6a)\end{aligned}$$

$$\begin{aligned}\overline{y}(\xi,\eta)&=r_1F_2(\xi,\eta)+r_2F_1(\eta,\xi)\\&-r_1F_2(\xi-\theta_1,\eta+\theta_1)-r_2F_3(\xi-\theta_1,\eta+\theta_1)\\&-r_2F_1(\eta-\theta_2,\xi+\theta_2)-r_1F_2(\eta-\theta_2,\xi+\theta_2)\\&+r_2F_3(\xi-\theta_1-\theta_2,\eta+\theta_1+\theta_2)\\&+r_1F_4(\xi-\theta_1-\theta_2,\eta+\theta_1+\theta_2). \quad (9.6b)\end{aligned}$$

We note that these functions are continuous in the whole domain of the cantilever. The Lamé functions A, B are given by

$$\begin{aligned}A(\xi,\eta)&=r_1G_0(\xi,\eta)+r_2G_1(\eta,\xi)-r_1G_0(\xi-\theta_1,\eta+\theta_1)\\&-r_2G_1(\xi-\theta_1,\eta+\theta_1)\\&-r_2G_1(\eta-\theta_2,\xi+\theta_2)-r_1G_2(\eta-\theta_2,\xi+\theta_2)\\&+r_2G_1(\xi-\theta_1-\theta_2,\eta+\theta_1+\theta_2)\\&+r_1G_2(\xi-\theta_1-\theta_2,\eta+\theta_1+\theta_2) \quad (9.7a)\end{aligned}$$

$$\begin{aligned}B(\xi,\eta)&=r_1G_1(\xi,\eta)+r_2G_0(\eta,\xi)-r_1G_1(\xi-\theta_1,\eta+\theta_1)\\&-r_2G_2(\xi-\theta_1,\eta+\theta_1)-r_2G_0(\eta-\theta_2,\xi+\theta_2)\\&-r_1G_1(\eta-\theta_2,\xi+\theta_2)\\&+r_2G_2(\xi-\theta_1-\theta_2,\eta+\theta_1+\theta_2)\\&+r_1G_3(\xi-\theta_1-\theta_2,\eta+\theta_1+\theta_2). \quad (9.7b)\end{aligned}$$

Both the Lame coefficients are continuous on the line GJ. Moreover, the following formula holds:

$$A(\alpha,\alpha-\theta_1)=0, \quad (9.8)$$

which means that the β lines are still tangent to the line GG_2.

To construct the functions $\Delta\overline{x}$, $\Delta\overline{y}$ and ΔA, ΔB within the domain HJH_2 we should make the change of variables $\beta \mapsto \alpha$, $\theta_1 \mapsto \theta_2$, $r_1 \mapsto r_2$, $\overline{x} \mapsto \overline{y}$ in the expressions referring to the domain GJG_2 to find

$$\begin{aligned}\Delta\overline{x}^{HJH_2}(\xi,\eta)&=r_1F_3(\eta-\theta_1-\theta_2,\xi+\theta_1+\theta_2)\\&+r_2F_4(\eta-\theta_1-\theta_2,\xi+\theta_1+\theta_2)\\\Delta\overline{y}^{HJH_2}(\xi,\eta)&=r_1F_2(\eta-\theta_1-\theta_2,\xi+\theta_1+\theta_2)\\&+r_2F_3(\eta-\theta_1-\theta_2,\xi+\theta_1+\theta_2)\\\Delta A^{HJH_2}(\xi,\eta)&=r_1G_2(\eta-\theta_1-\theta_2,\xi+\theta_1+\theta_2)\\&+r_2G_3(\eta-\theta_1-\theta_2,\xi+\theta_1+\theta_2)\\\Delta B^{HJH_2}(\xi,\eta)&=r_1G_1(\eta-\theta_1-\theta_2,\xi+\theta_1+\theta_2)\\&+r_2G_2(\eta-\theta_1-\theta_2,\xi+\theta_1+\theta_2). \quad (9.9)\end{aligned}$$

The Cartesian coordinates and the Lamé coefficients within HJH_2 are given by

$$\begin{aligned}\overline{x}^{HJH_2}(\xi,\eta)&=\overline{x}^{DHJG}(\xi,\eta)+\Delta\overline{x}^{HJH_2}(\xi,\eta)\\\overline{y}^{HJH_2}(\xi,\eta)&=\overline{y}^{DHJG}(\xi,\eta)+\Delta\overline{y}^{HJH_2}(\xi,\eta)\\A^{HJH_2}(\xi,\eta)&=A^{DHJG}(\xi,\eta)+\Delta A^{HJH_2}(\xi,\eta)\\B^{HJH_2}(\xi,\eta)&=B^{DHJG}(\xi,\eta)+\Delta B^{HJH_2}(\xi,\eta). \quad (9.10)\end{aligned}$$

On the line HH_2 (or $\beta=\alpha+\theta_2$) one finds

$$B(\alpha,\alpha+\theta_2)=0. \quad (9.11)$$

The α lines are tangent to the line HH_2. All the functions found are continuous on the line HJ.

10 Hencky net in the $JH_2J_2G_2$ domain

To construct the net one can make use of the Riemann formula by using the values of the unknown functions and their derivatives on the boundary lines. However, to make the derivation possibly brief we shall make use of some analogies, thus actually guessing the results. We sum up the functions defined in DHJG with functions of Chan's domains GJG_2 and HJH_2 of second rank (thus assuming their extrapolations):

$$\begin{aligned}
\overline{x}(\xi,\eta) &= \overline{x}^{DHJG}(\xi,\eta) + \Delta\overline{x}^{GJG_2}(\xi,\eta) + \Delta\overline{x}^{HJH_2}(\xi,\eta)\\
\overline{y}(\xi,\eta) &= \overline{y}^{DHJG}(\xi,\eta) + \Delta\overline{y}^{GJG_2}(\xi,\eta) + \Delta\overline{y}^{HJH_2}(\xi,\eta)\\
A(\xi,\eta) &= A^{DHJG}(\xi,\eta) + \Delta A^{GJG_2}(\xi,\eta) + \Delta A^{HJH_2}(\xi,\eta)\\
B(\xi,\eta) &= B^{DHJG}(\xi,\eta) + \Delta B^{GJG_2}(\xi,\eta) + \Delta B^{HJH_2}(\xi,\eta).
\end{aligned} \tag{10.1}$$

The final results read as follows:

$$\begin{aligned}
\overline{x}(\xi,\eta) &= r_1F_1(\xi,\eta) + r_2F_2(\eta,\xi) - r_1F_1(\xi-\theta_1,\eta+\theta_1) - r_2F_2(\xi-\theta_1,\eta+\theta_1)\\
&\quad -r_2F_2(\eta-\theta_2,\xi+\theta_2) - r_1F_3(\eta-\theta_2,\xi+\theta_2)\\
&\quad +r_2F_2(\xi-\theta_1-\theta_2,\eta+\theta_1+\theta_2) + r_1F_3(\xi-\theta_1-\theta_2,\eta+\theta_1+\theta_2)\\
&\quad +r_1F_3(\eta-\theta_1-\theta_2,\xi+\theta_1+\theta_2) + r_2F_4(\eta-\theta_1-\theta_2,\xi+\theta_1+\theta_2)\\
\overline{y}(\xi,\eta) &= r_1F_2(\xi,\eta) + r_2F_1(\eta,\xi) - r_1F_2(\xi-\theta_1,\eta+\theta_1) - r_2F_3(\xi-\theta_1,\eta+\theta_1)\\
&\quad -r_2F_1(\eta-\theta_2,\xi+\theta_2) - r_1F_2(\eta-\theta_2,\xi+\theta_2)\\
&\quad +r_2F_3(\xi-\theta_1-\theta_2,\eta+\theta_1+\theta_2) + r_1F_4(\xi-\theta_1-\theta_2,\eta+\theta_1+\theta_2)\\
&\quad +r_1F_2(\eta-\theta_1-\theta_2,\xi+\theta_1+\theta_2) + r_2F_3(\eta-\theta_1-\theta_2,\xi+\theta_1+\theta_2)\\
A(\xi,\eta) &= r_1G_o(\xi,\eta) + r_2G_1(\eta,\xi) - r_1G_0(\xi-\theta_1,\eta+\theta_1) - r_2G_1(\xi-\theta_1,\eta+\theta_1)\\
&\quad -r_2G_1(\eta-\theta_2,\xi+\theta_2) - r_1G_2(\eta-\theta_2,\xi+\theta_2)\\
&\quad +r_2G_1(\xi-\theta_1-\theta_2,\eta+\theta_1+\theta_2) + r_1G_2(\xi-\theta_1-\theta_2,\eta+\theta_1+\theta_2)\\
&\quad +r_1G_2(\eta-\theta_1-\theta_2,\xi+\theta_1+\theta_2) + r_2G_3(\eta-\theta_1-\theta_2,\xi+\theta_1+\theta_2)\\
B(\xi,\eta) &= r_1G_1(\xi,\eta) + r_2G_0(\eta,\xi) - r_1G_1(\xi-\theta_1,\eta+\theta_1) - r_2G_2(\xi-\theta_1,\eta+\theta_1)\\
&\quad -r_2G_0(\eta-\theta_2,\xi+\theta_2) - r_1G_1(\eta-\theta_2,\xi+\theta_2)\\
&\quad +r_2G_2(\xi-\theta_1-\theta_2,\eta+\theta_1+\theta_2) + r_1G_3(\xi-\theta_1-\theta_2,\eta+\theta_1+\theta_2)\\
&\quad +r_1G_1(\eta-\theta_1-\theta_2,\xi+\theta_1+\theta_2) + r_2G_2(\eta-\theta_1-\theta_2,\xi+\theta_1+\theta_2).
\end{aligned} \tag{10.2}$$

Exemplary cantilever comprising the $JH_2J_2G_2$ domain is depicted in Fig. 20.

11 Geometry of further subdomains of longer cantilevers

The construction of Hencky nets shown in the previous sections can be continued without any limitations (cf. Fig. 21a,b). Thus, one can find the nets of fibres of cantilevers of any length. This extension is shown below for the case of r_1=r_2=r. The additional terms for Chan-like domains of rank n in the lower zone can be put in the form

$$\begin{aligned}
\frac{\Delta\overline{x}_d^n}{r} &= (-1)^n F_n(\alpha-n\theta,\beta+n\theta)\\
&\quad +(-1)^n F_{n+1}(\alpha-n\theta,\beta+n\theta).
\end{aligned} \tag{11.1}$$

The increment of y can be found by differentiating the formula above with using (a.4):

$$\begin{aligned}
\frac{\Delta\overline{y}_d^n}{r} &= (-1)^n F_{n+1}(\alpha-n\theta,\beta+n\theta)\\
&\quad +(-1)^n F_{n+2}(\alpha-n\theta,\beta+n\theta).
\end{aligned} \tag{11.2}$$

Similarly, the additional terms for the upper Chan-like domains are given by the following change of variables:

$$\Delta\overline{y}_g^n(\xi,\eta) = \Delta\overline{x}_d^n(\eta,\xi), \qquad \Delta x_g^n(\xi,\eta) = \Delta y_d^{-n}(\eta,\xi). \tag{11.3}$$

Thus, we have

$$\begin{aligned}
\frac{\Delta\overline{x}_g^n}{r} &= (-1)^n F_{n+1}(\beta-n\theta,\alpha+n\theta)\\
&\quad +(-1)^n F_{n+2}(\beta-n\theta,\alpha+n\theta)\\
\frac{\Delta\overline{y}_g^n}{r} &= (-1)^n F_n(\beta-n\theta,\alpha+n\theta)\\
&\quad +(-1)^n F_{n+1}(\beta-n\theta,\alpha+n\theta).
\end{aligned} \tag{11.4}$$

The geometry of nets in the middle domain of rank n of the cantilever is given by the following recurrence formulae:

$$\begin{aligned}
\overline{x}^n &= \overline{x}^{n-1} + \Delta\overline{x}_d^{n-1} + \Delta\overline{x}_g^{n-1},\\
\overline{y}^n &= \overline{y}^{n-1} + \Delta\overline{y}_d^{n-1} + \Delta\overline{y}_g^{n-1} \quad n \geq 2.
\end{aligned} \tag{11.5}$$

The Lamé functions $A(\alpha,\beta)$ and $B(\alpha,\beta)$ can be found by the mnemonic method described in Section 8. For the lower

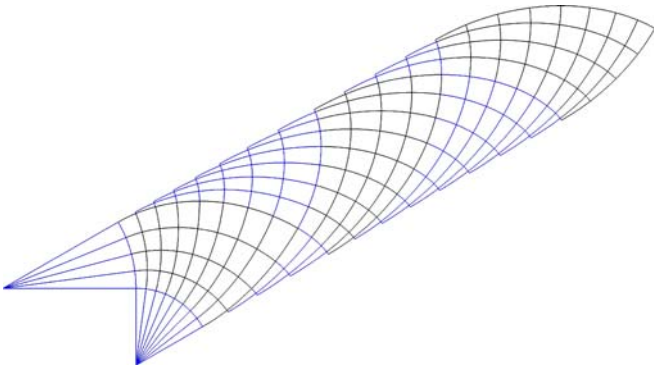

Fig. 20 Michell cantilever, $\kappa = 3$, $\theta_1 = \frac{\pi}{3}$, $\theta_2 = \frac{\pi}{6}$, $\alpha_p = \frac{5\pi}{6}$, $\beta_p = \frac{2\pi}{3}$

straight boundary line we must assure that $A(\alpha, \alpha-\theta)=0$, while on the upper line, we shall have $B(\alpha, \alpha+\theta)=0$.

12 Final remarks

The paper proves that in the problem considered the parametric lines of the Hencky net and Lamé coefficients are expressed in terms of closed formulae involving Lommel-like functions. In other problems this property might not be necessarily the case; therefore, we should use other available methods, like those developed, e.g., in Dewhurst and Collins (1973) and Dewhurst (2001).

Appendix A

The following new integration results are used in the paper ($n \geq 0$):

$$\int_0^{\lambda} \cos(\lambda - \alpha) G_1(\mu, \alpha) d\alpha = \cos(\mu - \lambda) - \cos\lambda + F_2(\mu, \lambda), \quad \text{(A.1)}$$

$$\int_0^{\lambda} \sin(\lambda - \alpha) G_1(\mu, \alpha) d\alpha = \sin\lambda + \sin(\mu - \lambda) - F_1(\mu, \lambda), \quad \text{(A.2)}$$

$$\int_{\theta}^{\xi} \alpha \cos(\xi - \alpha) G_n(\alpha - \theta, \eta + \theta) d\alpha$$
$$= (n+1) F_{n+2}(\xi - \theta, \eta + \theta) + (\eta + \theta) F_{n+3}(\xi - \theta, \eta + \theta)$$
$$+ \theta F_{n+1}(\xi - \theta, \eta + \theta), \quad \text{(A.3)}$$

$$\int_{\theta}^{\xi} \alpha \sin(\xi - \alpha) G_n(\alpha - \theta, \eta + \theta) d\alpha$$
$$= (n+1) F_{n+3}(\xi - \theta, \eta + \theta) + (\eta + \theta) F_{n+4}(\xi - \theta, \eta + \theta)$$
$$+ \theta F_{n+2}(\xi - \theta, \eta + \theta), \quad \text{(A.4)}$$

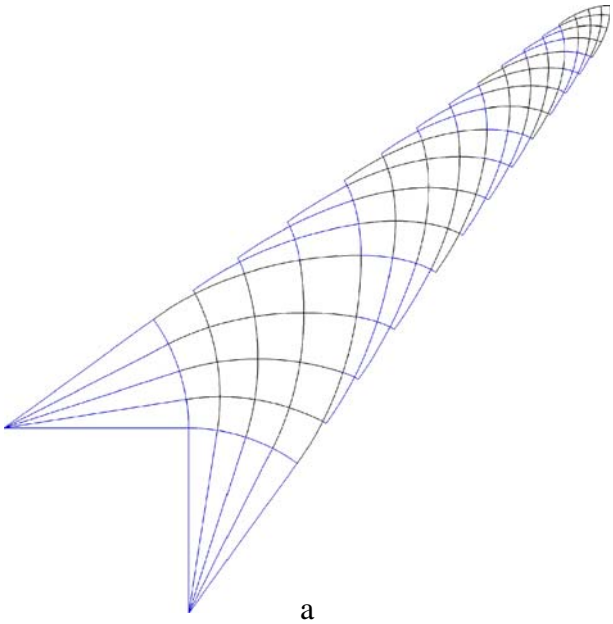

a

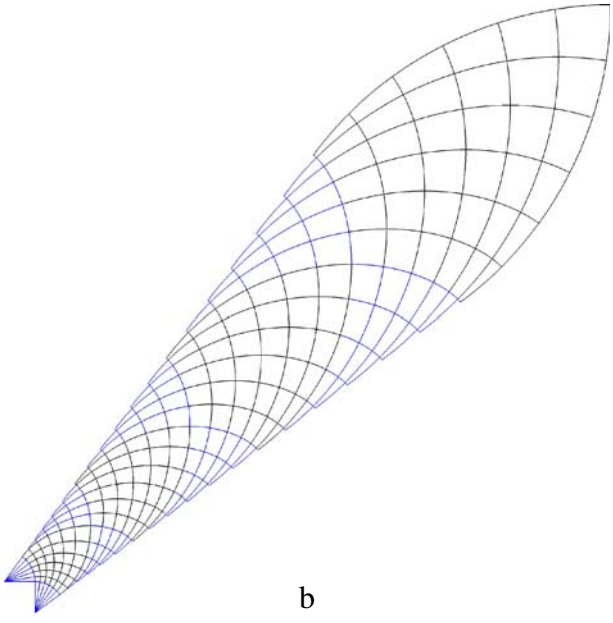

b

Fig. 21 **a** Michell cantilever, $\kappa = 1$, $\theta_1 = \frac{\pi}{5}$, $\theta_2 = \frac{\pi}{5}$, $\alpha_p = \frac{4\pi}{5}$, $\beta_p = \frac{4\pi}{5}$. **b** Michell cantilever, $\kappa = 1$, $\theta_1 = \frac{3\pi}{10}$, $\theta_2 = \frac{3\pi}{10}$, $\alpha_p = \frac{6\pi}{5}$, $\beta_p = \frac{6\pi}{5}$

$$\int_0^{t} D_0(x, t-x) dx = \sin t, \quad \text{(A.5)}$$

$$\int_{\theta_1}^{\lambda} G_0(\lambda - \alpha, \mu) G_{n-1}(\alpha - \theta_1, \theta_2) d\alpha$$
$$= G_n(\lambda - \theta_1, \mu + \theta_2) - \delta_{n0} G_0(\lambda - \theta_1, \mu), \quad \text{(A.6)}$$

where $\delta_{00}=1$ and $\delta_{n0}=0$ if $n=1,2,\ldots$.

The result (A3) is sometimes used in the form

$$\int_{\theta}^{\eta} \beta\cos(\eta-\beta)G_n(\beta-\theta,\xi+\theta)d\beta$$
$$= (n+1)\,F_{n+2}(\eta-\theta,\xi+\theta)+(\xi+\theta)F_{n+3}(\eta-\theta,\xi+\theta)$$
$$+\theta F_{n+1}(\eta-\theta,\xi+\theta). \qquad (A.3')$$

To prove (A5) it is sufficient to apply the Laplace transform L_t and make use of (a.174).

Appendix B: derivation of the formula (7.5)

Let a function w satisfy the equation $Lw=f$ within the domain QFE, parameterized by (α,β) (see Fig. 13); here, L is the operator given by (6.3), and f is a given function of two variables given in the same domain. Let us define the function D_0 by (7.7). For given (ξ,η) we define

$$G(\alpha,\beta)=D_0(\alpha-\xi,\eta-\beta) \qquad (B.1)$$

and note that $LG=0$.Within the domain QFE, $\alpha-\xi\geq 0,\ \eta-\beta\geq 0$ (see Fig. 13). Making use of (a.20)–(a.22) we find the identity

$$2\int_{\Omega} fG\,d\alpha\,d\beta=\int_{\partial\Omega}\left(-G\frac{\partial w}{\partial\alpha}+w\frac{\partial G}{\partial\alpha}\right)d\alpha+\int_{\partial\Omega}\left(G\frac{\partial w}{\partial\beta}-w\frac{\partial G}{\partial\beta}\right)d\beta, \qquad (B.2)$$

where Ω=QFE. The above identity holds for $w(\alpha,\beta)=\overline{x}(\alpha,\beta)$ and f=0, see (a.56). By using the properties

$$G(\alpha,\eta)=1,\quad G(\xi,\beta)=1\,, \qquad (B.3)$$

we perform the integration

$$\int_{QF}\left(-G\frac{\partial\overline{x}}{\partial\alpha}+\overline{x}\frac{\partial G}{\partial\alpha}\right)d\alpha=\overline{x}_Q-\overline{x}_F \qquad (B.4a)$$

$$\int_{EQ}\left(G\frac{\partial\overline{x}}{\partial\beta}-\overline{x}\frac{\partial G}{\partial\beta}\right)d\beta=\overline{x}_Q-\overline{x}_E \qquad (B.4b)$$

and rearrange the integral over FE

$$\int_{FE}\left(-G\frac{\partial\overline{x}}{\partial\alpha}+\overline{x}\frac{\partial G}{\partial\alpha}\right)d\alpha+\int_{FE}\left(G\frac{\partial\overline{x}}{\partial\beta}-\overline{x}\frac{\partial G}{\partial\beta}\right)d\alpha=\int_{\xi}^{\eta+\theta_1}\left[\overline{x}(\alpha,\alpha-\theta_1)\left(\frac{\partial G}{\partial\beta}-\frac{\partial G}{\partial\alpha}\right)_{|\beta=\alpha-\theta_1}+G(\alpha,\alpha-\theta_1)\left(\frac{\partial\overline{x}}{\partial\alpha}-\frac{\partial\overline{x}}{\partial\beta}\right)_{|\beta=\alpha-\theta_1}\right]d\alpha. \qquad (B.4c)$$

Thus, (B.2) gives the value $\overline{x}$ at point Q of coordinates (ξ,η)

$$\overline{x}(\xi,\eta)=\frac{1}{2}(\overline{x}_F+\overline{x}_E)-\frac{1}{2}\int_{\xi}^{\eta+\theta_1}\overline{x}(\alpha,\alpha-\theta_1)\left(\frac{\partial G}{\partial\beta}-\frac{\partial G}{\partial\alpha}\right)_{|\beta=\alpha-\theta_1}d\alpha-\frac{1}{2}\int_{\xi}^{\eta+\theta_1}G(\alpha,\alpha-\theta_1)\varphi(\alpha)d\alpha, \qquad (B.5)$$

where $\varphi(\alpha)$ is given by (7.6). Now we make use of $\overline{x}$ being constant on CG see (7.4)

$$\overline{x}_E=\overline{x}_F=\overline{x}(\alpha,\alpha-\theta_1)=r_1\sin\theta_1 \qquad (B.6)$$

and simplify (B.5) to the form

$$\overline{x}(\xi,\eta)=r_1\sin\theta_1\left[1-\frac{1}{2}g(\xi,\eta)\right]-\frac{1}{2}\int_{\xi}^{\eta+\theta_1}G(\alpha,\alpha-\theta_1)\varphi(\alpha)d\alpha, \qquad (B.7)$$

where

$$g(\xi,\eta)=\int_{\xi}^{\eta+\theta_1}\left(\frac{\partial G}{\partial\beta}-\frac{\partial G}{\partial\alpha}\right)_{|\beta=\alpha-\theta_1}d\alpha. \qquad (B.8)$$

By using the known rule $dJ_0(z)/dz=-J_1(z)$ one can rearrange (B.8) to the form

$$g(\xi,\eta)=\int_{\xi}^{\eta+\theta_1}\frac{\eta+\theta_1-\xi}{(\alpha-\xi)^{1/2}(\eta+\theta_1-\xi)^{1/2}}\times J_1\left(2(\alpha-\xi)^{1/2}(\eta+\theta_1-\xi)^{1/2}\right)d\alpha. \qquad (B.9)$$

We recall the known integration result (see Chan 1967, (13))

$$\int_0^t\frac{t}{2x^{1/2}(t-x)^{1/2}}J_1\left(2x^{1/2}(t-x)^{1/2}\right)dx=1-\cos t \qquad (B.10)$$

and find

$$g(\xi,\eta)=2[1-\cos(\eta+\theta_1-\xi)]. \qquad (B.11)$$

Substitution of (B.11) into (B.7) gives (7.5).

References

Chan HSY (1967) Half-plane slip-line fields and Michell structures. Q J Mech Appl Math 20:453–469

Dewhurst P (2001) Analytical solutions and numerical procedures for minimum-weight Michell structures. J Mech Phys Solids 49:445–467

Dewhurst P, Collins IF (1973) A matrix technique for constructing slip-line field solutions to a class of plane strain plasticity problems. Int J Numer Methods Eng 7:357–378

Graczykowski C, Lewiński T (2003) Optimal Michell's cantilever transmitting a given point load to a circular support. Analysis of the exact solution. In: Szcześniak W (ed) Theoretical foundations of civil engineering-XI. Oficyna Wydawnicza PW, Warsaw, pp 351–368

Graczykowski C, Lewiński T (2005) The lightest plane structures of a bounded stress level, transmitting a point load to a circular support. Control Cybern 34:227–253

Hemp WS (1973) Optimum structures. Clarendon, Oxford

Hill R (1950) The mathematical theory of plasticity. Clarendon, Oxford

Lewiński T (2004) Michell structures formed on surfaces of revolution. Struct Multidisc Optim 28:20–30

Lewiński T, Telega JJ (2000) Plates, laminates and shells. Asymptotic analysis and homogenisation. World Scientific, Singapore

Lewiński T, Telega JJ (2001) Michell-like grillages and structures with locking. Arch Mech 53:303–331

Lewiński T, Zhou M, Rozvany GIN (1994a) Extended exact solutions for least-weight truss layouts—Part I: cantilever with a horizontal axis of symmetry. Int J Mech Sci 36:375–398

Lewiński T, Zhou M, Rozvany GIN (1994b) Extended exact solutions for least-weight truss layouts—Part II: unsymmetric cantilevers. Int J Mech Sci 36:399–419

Michell AGM (1904) The limits of economy of material in frame-structures. Philos Mag 8:589–597

Prager W (1959) On a problem of optimal design. In: Olszak W (ed) Proceedings of IUTAM Symposium on non-homogeneity in elasticity and plasticity. Pergamon, London, pp 125–132

Prager W (1978a) Nearly optimal design of trusses. Comput Struct 8:451–454

Prager W (1978b) Optimal layout of trusses of finite number of joints. J Mech Phys Solids 26:241–250

Rozvany GIN (1997a) Some shortcomings in Michell's truss theory. Struct Optim 1996, 12:244–250; 1997, 13:203–204

Rozvany GIN (1997b) Partial relaxation of the orthogonality requirement for the classical Michell truss. Struct Optim 13:271–274

Selyugin SV (2004) Some general results for optimal structures. Struct Multidisc Optim 26:357–366

Strang G, Kohn RV (1983) Hencky–Prandtl nets and constrained Michell trusses. Comput Methods Appl Mech Eng 36:207–222